Novel Tetrahydropyrido[1,2-a]isoindolone Derivatives (Valmerins): Potent Cyclin-Dependent Kinase/Glycogen Synthase Kinase 3 Inhibitors with Antiproliferative Activities and Antitumor Effects in Human Tumor Xenografts

Rajâa Boulahjar,[†,‡] Aziz Ouach,[†] Chiurato Matteo,[†] Stephane Bourg,[†] Myriam Ravache,[⊥] Rémy le Guével,[⊥] Séverine Marionneau,[#] Thibauld Oullier,[#] Olivier Lozach,[§] Laurent Meijer,[∥,§] Christiane Guguen-Guillouzo,[⊥] Saïd Lazar,[‡] Mohamed Akssira,[‡] Yves Troin,[±] Gérald Guillaumet,[†] and Sylvain Routier*,[†]

[†]Institut de Chimie Organique et Analytique, Université d'Orléans, UMR CNRS 7311, rue de Chartres, BP 6759, 45067 Orléans Cedex 2, France

[‡]Laboratoire de Chimie, Bioorganique et Analytique, URAC 22 pôle Répam, Université Hassan II Mohammedia-Casablanca, BP 146, 28800 Mohammedia, Morocco

[§]CNRS, "Protein Phosphorylation & Human Disease" group, USR3151, Station Biologique, B.P. 74, 29682 Roscoff Cedex, France

[∥]ManRos Therapeutics, Centre de Perharidy, 29680 Roscoff, France

[⊥]Plateforme ImPACcell-SFR BIOSIT UMS-CNRS3480 UMS-INSERM018, Université de Rennes 1, 35043 Rennes Cedex, France.

[#]In vivo Platform, Cancéropôle Grand Ouest, 63 quai Magellan, 44000 Nantes, France

[±]Clermont Université, ENSCCF, Laboratoire de Chimie des Hétérocycles et des Glucides, BP 10448, 63000 Clermont-Ferrand, France

Ⓢ *Supporting Information*

ABSTRACT: The development of CDK and GSK3 inhibitors has been regarded as a potential therapeutic approach, and a substantial number of diverse structures have been reported to inhibit CDKs and GSK-3β in recent years. Only a few molecules have gone through or are currently undergoing clinical trials as CDK and GSK inhibitors. In this paper, we prepared valmerins, a new family containing the tetrahydropyrido[1,2-a]isoindone core. The fused heterocycle was prepared with a straightforward synthesis that was functionalized by a (het)arylurea. Twelve valmerins inhibited the CDK5 and GSK3 with an IC$_{50}$ < 100 nM. A semiquantitative kinase scoring was realized, and a cellular screening was done. At the end of our study, we investigated the in vivo potency of one valmerin. Mice exhibited good tolerance to our lead, which proved its efficacy and clearly blocked tumor growth. Valmerins appear also as good candidates for further development as anticancer agents.
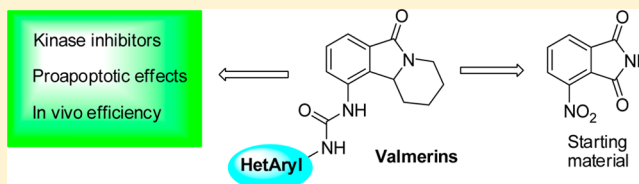
■ INTRODUCTION

Abnormal protein phosphorylation is frequently involved in the development of various human pathogeneses. Among the 518 human genes encoding protein kinases, cyclin-dependent protein kinases (CDKs) and glycogen synthase kinase-3 (GSK3), two serine/threonine kinases, have attracted considerable attention because of their frequent deregulation in major pathologies. CDKs are located in the nucleus and participate mainly in processes of cell cycle control, transcription, and post-transcriptional modifications but also in cell differentiation and cancer cell death.[1,2] Consequently, many pharmacological inhibitors of CDKs have been found to display promising antitumor and/or neuroprotective activities. Although a few kinase inhibitors display a definite specificity profile, many of them are rather unselective and inhibit several kinases such as

GSK3. This enzyme, which is encoded by two independent genes, -α and -β, is interestingly involved in a broad range of biological processes such as stem-cell renewal, the cell-division cycle, differentiation, apoptosis, circadian rhythm, transcription, and insulin action, and its deregulation has been associated with many diseases, such as metabolic disorders, CNS diseases, and cancer.[3,4]

The development of CDK and GSK3 inhibitors has been regarded as a potential therapeutic approach and a substantial number of diverse structures have been reported to inhibit CDKs and GSK-3β in recent years. Only a few molecules have gone through or are currently undergoing clinical trials. Flavopiridol (Alvocidib) and its analogues P276-00, (R)-roscovitine
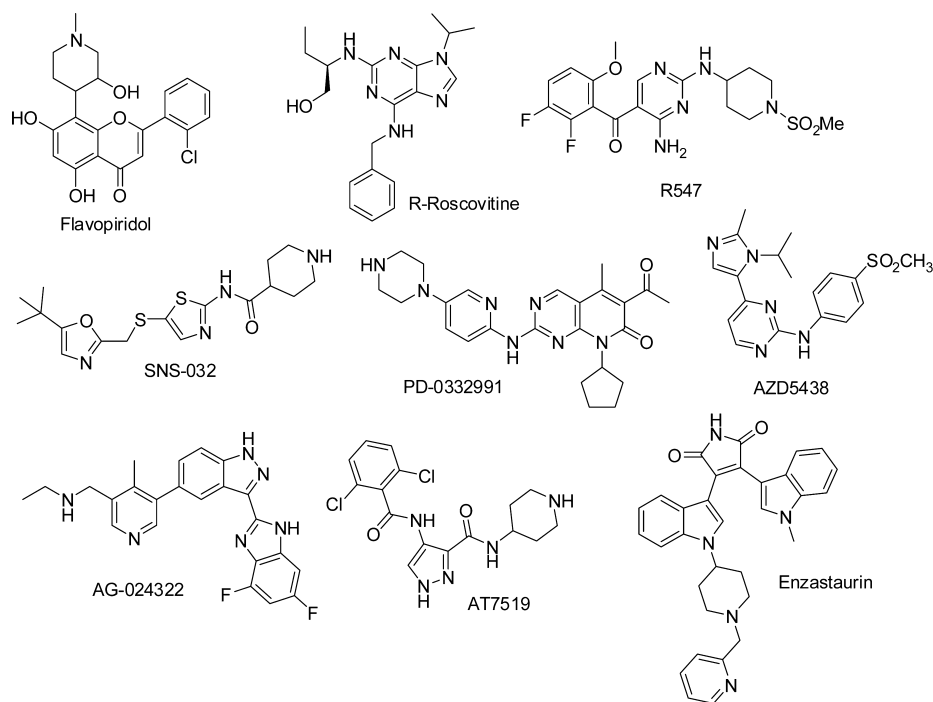
Figure 1. Some representative CDK and GSK3 inhibitors in clinical trials.
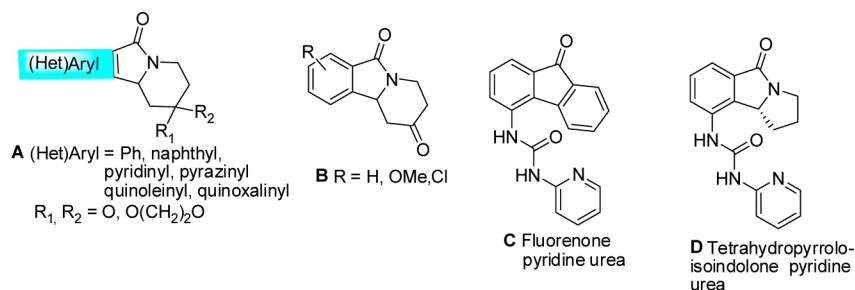

Figure 2.

(Seliciclib), R547, SNS-032, PD-0332991 (CDK4 and -6 selectivity), AZD5438, AG-024322, and AT7519 are representative examples (Figure 1).[5−12] Most of them target multiple CDKs and are applied in the treatment of leukemia, melanoma and solid tumors. Only nine GSK3β inhibitors are in development, while the bis(indolylmaleimide) derivative named enzastaurin (LY317615, phase II) is appropriate for brain cancer.[13]

In the search for heterocyclic skeletons that could be used to design new protein kinase inhibitors, we first developed novel indolocarbazole analogues and published original anticancer series possessing strong cell effects and exhibiting kinase inhibition.[14] Some of them have entered clinical trials. More recently, we reported an original synthesis leading to het(aryl)indolizinones **A** via an (acyl)iminium intermediate (Figure 2).[15] Thus, we envisioned the use of our optimized synthetic pathway leading to tetrahydropyrido[1,2-a]isoindolone **B** as the central core for new CDK inhibitors. To establish our SAR studies, we will start from the work of Honma et al. which described new bis(het)aryl ureas **C** and **D** to optimize their selective CDK4 inhibitors.[16]

Our chemical investigations indicated that the derivatives **A** are readily available by condensation of a β-formylbenzoic acid with a primary amine (i.e., 2-(2-methyl-1,3-dioxolan-2-yl)ethanamine)[17]

or from a β-hydroxylactam under intramolecular cyclization. In our opinion, synthesis of the valmerins[18] (i.e., tetrahydropyrido-[1,2-a]isoindolone(hetaryl)ureas) **E** will also be achieved using as a key step the intramolecular cyclization of the β-hydroxylactam **4** which is readily accessible from the nitrophthalimide **1** (Scheme 1).

Scheme 1. Retrosynthetic Scheme
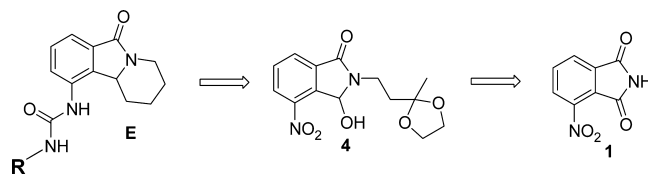
A complete SAR study was carried out using various urea residues on **E** (alkyls, aryls, and heteroaryls) to afford a very interesting library exhibiting highly potent CDK/GSK3 inhibitors.[19] The best final derivatives were next evaluated against seven cancer cell lines, and, after selection we used our leader for in vivo evaluations on xenograft mice. The results, from synthesis to a full biological evaluation, are also described in this paper.

Scheme 2[a]
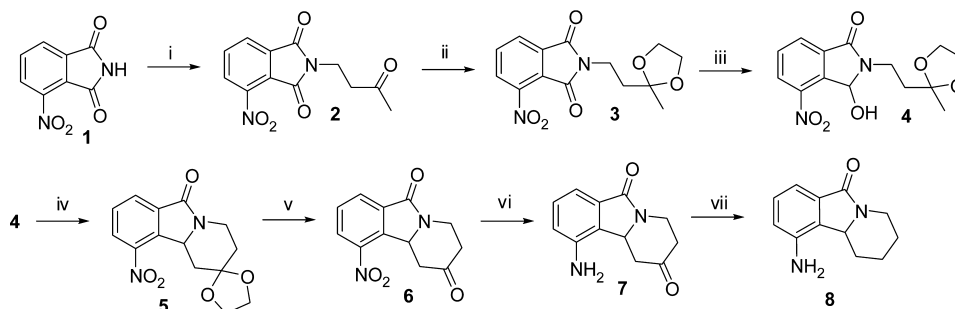
[a]Key: (i) methyl vinyl ketone (1.2 equiv), Triton B (cat.), EtOAc, reflux, 12 h, 85%; (ii) ethylene glycol (2.0 equiv), PTSA·H$_2$O (cat.), toluene, Dean–Stark, reflux, 12 h, 89%; (iii) NaBH$_4$ (3.0 equiv), THF/MeOH (1/2), −20 °C, 15 min, 76% ; (iv) PTSA·H$_2$O (0.5 equiv), toluene, Dean–Stark, reflux, 6 h, 73%; (v) HCl 10%, acetone, reflux, 3 h, 90%; (vi) Pd/C (10%), H$_2$ P$_{atm}$, CH$_2$Cl$_2$, rt, 16 h, 88%; (vii) NH$_2$−NH$_2$·H$_2$O (4.0 equiv), Na (3.0 equiv), ethylene glycol, reflux, 4 h, 86%.

■ CHEMISTRY

Only a few studies are related to the synthesis of the targeted tetrahydropyrido[1,2-*a*]isoindolone core.[20,21] In our work, we envisioned that the attempted scaffold **E** could be produced from the commercially available 3-nitrophthalimide **1** after a four-step sequence.

A Michael addition was first carried out with **1** (Scheme 2) and the methyl vinyl ketone in the presence of a catalytic amount of Triton B. After 12 h, the ketone **2** (85%) was isolated and then protected by treatment with ethylene glycol in refluxing toluene to afford the cyclic ketal **3** in 89% yield. A regioselective reduction of the maleimide group was carried out at low temperature with an excess of NaBH$_4$ in only a few minutes. The choice of the solvent and the strict control of temperature are important experimental criteria to obtain the desired selectivity. Formation of the other regioisomer was never observed in these conditions. The cyclization of the hydroxylactam **4** was promoted using PTSA hydrate at toluene reflux and led to the tetrahydropyrido[1,2-*a*]isoindolone core after a few hours in an acceptable 73% yield. The change in the amount of PTSA or the use of another acidic source (i.e., BF$_3$·Et$_2$O, HCl, or CSA) led only to lower yields.

Once the cycloadduct **5** had been obtained, the ketone protection was removed using an aqueous hydrochloride solution in refluxing acetone in 90% yield. The selective reduction of the nitro group of **6** was successfully accomplished using hydrogenolysis at room temperature in CH$_2$Cl$_2$. This method led to the aniline **7** in 88% yield. Finally, we carried out a modified Wolff−Kishner reaction with hydrazine and sodium in refluxing ethylene glycol which furnished the key amine **8** in 86% yield.[22] Direct conversion of **6** into **8** under hydrogen pressure at high temperature failed. Ketone could be reduced prior to the nitro group, but lower yields decrease the interest of this route.

Starting from **8**, classical urea formation involving triphosgene or *p*-nitrophenyl carbamate methods gave disappointing results, the low reactivity of the amine leading only to complex mixtures. We therefore focused our efforts on Curtius rearrangements. Starting from highly available acids in aliphatic, aromatic, and heteroaromatic series, the isocyanides were first generated in situ and immediately scavenged by our prebuilt amine **8**. This very attractive "one-pot" general procedure (Scheme 3) was applied to several acids **F** to furnish the attempted valmerin ureas **E**.

Scheme 3[a]
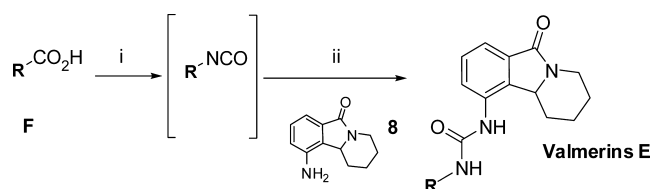
[a]Key: (i) (a) Et$_3$N (1.3 equiv), −10 °C, THF, 5 min, (b) ClCO$_2$Et (1.5 equiv), −10 °C, THF, 2 h, (c) NaN$_3$ (1.7 equiv), −10 °C, H$_2$O, 1 h, (d) toluene, reflux, 1 h; (ii) **8**, toluene, reflux, 24 h, valmerins 13–40, 42–90% yields.

To provide the dissymmetrical urea library, we used 23 commercially available acids reported in Table 1. Others are readily available after some chemical transformations (Scheme 4).[23−25] To prepare the MOM-protected pyridine and quinoleine derivatives **9−12**, we started from the corresponding hydroxy acids which were first transformed into methyl esters prior to conducting MOM protection. At the end of the sequence, a simple saponification led to the expected compounds. Overall yields of the three-step syntheses were in the 70−77% yield range.

Finally, the isocyanates corresponding to 27 carboxylic acids were formed and quenched in situ by amine **8** to afford the ureas **13−39**. Products were isolated in 42−90% yields, which mainly depended on the nature and solubility of carboxylic acids.
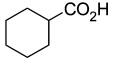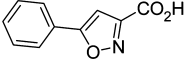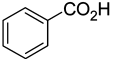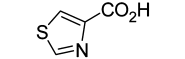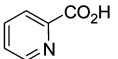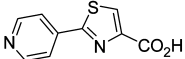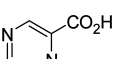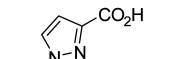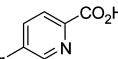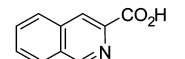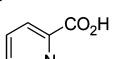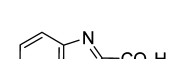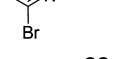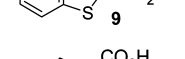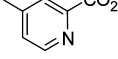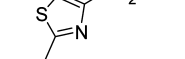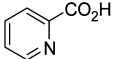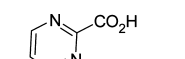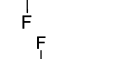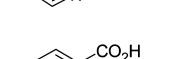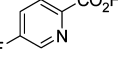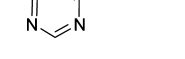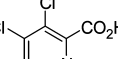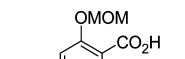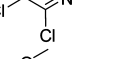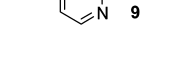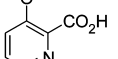
The sole limitation we found concerned the use of 1*H*-pyrazole-3-carboxylic acid, which led via Curtius rearrangement and in situ condensation with the amine **8** to valmerin **40** in a very poor 4% yield (Scheme 5).

Alternatively, we condensed in situ the *N*-1-Boc-3-aminopyrazole[16] and the isocyanate of **8** which was quantitatively formed using BTC in the presence of Et$_3$N. After 16 h, the attempted urea **41** was isolated in 56% yield. Boc deprotection was carried out in basic media to furnish **40** at room temperature in a satisfying 66% yield. The MOM protective groups of **36−39** were next removed under classical media to afford the final derivatives **42−45** in high yields.

■ RESULTS AND DISCUSSION

Kinase Assays. First we tested our valmerin library against several representative kinases in order to determine the influence of urea R residues (Table 2) on kinase inhibition

Table 1. Synthesis of Valmerins E from Acids F via Curtius Rearrangement

Entry	Acids F	Valmerins E (yield %)[a]	Entry	Acids F	Valmerins E (yield %)[a]
1		13 (86%)	15		27 (87%)
2		14 (80%)	16		28 (62%)
3		15 (90%)	17		29 (60%)
4		16 (70%)	18		30 (62%)
5		17 (66%)	19		31 (71%)
6		18 (70%)	20		32 (50%)
7		19 (80%)	21		33 (42%)
8		20 (70%)	22		34 (87%)
9		21 (73%)	23		35 (76%)
10		22 (60%)	24		36 (73%)
11		23 (70%)	25		37 (78%)
12		24 (81%)	26		38 (75%)
13		25 (79%)	27		39 (70%)
14		26 (72%)			

[a]Yields are indicated in isolated products.

(CDK5/p25, GSK3α/β, and DYRK1A). With an alkyl and phenyl group, the valmerins **13** and **14** are inactive (entries 1 and 2) on all three kinases. All other compounds exhibited a kinase inhibitory effect, and structural modifications led to a modulation in their activity.

The structural key that allows interaction with the kinase active site is the presence of a nitrogen atom on the aromatic ring in position 2. Compound **15** (entry 3) inhibited CDK5 at IC$_{50}$ = 80 nM. This result confirms the crucial role of the pyridine nitrogen atom in position 2,[16] which could be explained by the formation of an intramolecular hydrogen bond between the pyridinic nitrogen atom and a labile urea hydrogen atom. The resulting rigidity and withdrawal of

the valmerins led to a maximal occupation of the ATP pocket.

Adding a second electron-rich and basic nitrogen atom to the heteroaromatic residue of urea maintained this effect, and the activity of pyrazine **16** increased to 70 nM for each kinase, but this strategy is worthwhile only for the 5 position. Displacement of the second nitrogen (i) from position 4 to 5 (for number assignment see general formula table 3) led to the quite inactive pyrimidine compound **34** and (ii) from position 4 to 3 a micromolar active derivative **35** (entries 22 and 23) was obtained.

A contraction ring prompted us to use the thiazole, pyrazole, and oxazole heterocycles, but each synthesized valmerin

Scheme 4[a]
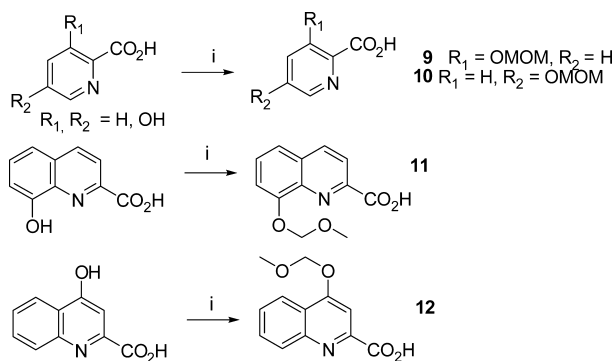
[a]Key: (i) (a) MeOH, SOCl$_2$ (1.5 equiv), 60 °C, 16 h, (b) K$_2$CO$_3$ (2.0 equiv), MOMCl (1.5 equiv), acetone, reflux, 16 h, (c) NaOH (1.2 equiv), THF/H$_2$O (1/1), rt, 2 h, **9** 75%, **10** 77%, **11** 70%, **12** 72%.

showed a lack of activity (entries 7−13). Submicromolar active compounds are the less substituted **28**, **30**, and **33**. Interestingly, the more basic pyrazole containing product **40** led to the best activity, but a simple methylation increased the IC$_{50}$ by a factor of 5 (entry 10 vs 11), therefore decreasing the interest of this substitution.

The last modification we tried was the use of fused bicyclic heterocycles. Benzothiazole **32** was poorly active, but fortunately, the isoquinoline valmerin **31** gave interesting results and activities on CDK5 that are comparable to valmerins **15** and **16** (entries 3 and 4). Nevertheless, hydroxyquinolines **44** and **45** did not have any effect on the kinases.

Valmerins exhibited some selectivity in kinase inhibition. All of them were quite inactive on DYRK1A, but a good inhibition of GSK3 was observed. Except for valmerins **32** and **45**, all the other derivatives displayed an IC$_{50}$ in the submicromolar range.

In general, the GSK3 (compared to CDK5) active site accepts bulkier groups.[27] CDK5-inactive **26**, **27**, **29**, and **35** derivatives appeared to be potent against GSK3 with IC$_{50}$ ranging between 130 and 330 nM. The most selective compound is without doubt valmerin **34**, which is completely inactive on CDK5 and DYRK1A (IC$_{50}$> 10 μM) but exhibits a 750 nM IC$_{50}$ on GSK3.

The three valmerins **15**, **16**, and **31** emerged as good leads to pursue our investigations. Among them, we selected the pyridine ring to explore other avenues and complete our QSAR studies (Table 3). We added CK1 to our enzyme panel. We also showed that valmerin **15** (entry 1) and **16** (not shown) similarly affect the three structurally related kinases CDK 1, 5 and GSK3. All of the new derivatives have only moderate interactions with CK1 and DYRK1A active sites, while major effects are always observed on CDK5 and GSK3.
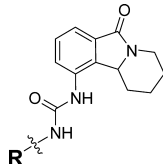
On CDK5, a bulky and electron-rich bromo atom enhanced the activity. Positions 2 and 4 were privileged compared to position 3 (entries 2−4). Valmerins **18** and **19** exhibited remarkable IC$_{50}$ values of 40 and 25 nM, respectively.
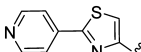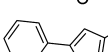
A slight decrease in kinase inhibition occurred when bromine was replaced by a fluorine atom (entries 5 and 2), but with this small atom, valmerin **20** was as active as the previously selected compound **15**. A poly chloration or an increase in the substitution size (i.e., piperidine or a phenyl groups, entries 7, 9, and 10) led to a full inactivation of valmerins against CDK5. In position 3, valmerins could create a supplementary hydrogen bond with the active site. Adding a hydroxyl group in this position led to derivative **42**, which inhibits CDK5 with an IC$_{50}$ of 37 nM. This hydrophilic group is nevertheless a handicap in position 5 since it may interact with the urea function and dramatically perturb the crucial orientation of the pyridine ring (entry 14).

As mentioned previously, the GSK3 active site accepts more variations and the presence of lipophilic and hydrophilic groups is well tolerated. Five valmerins **17−20** and **42** showed IC$_{50}$

Scheme 5[a]
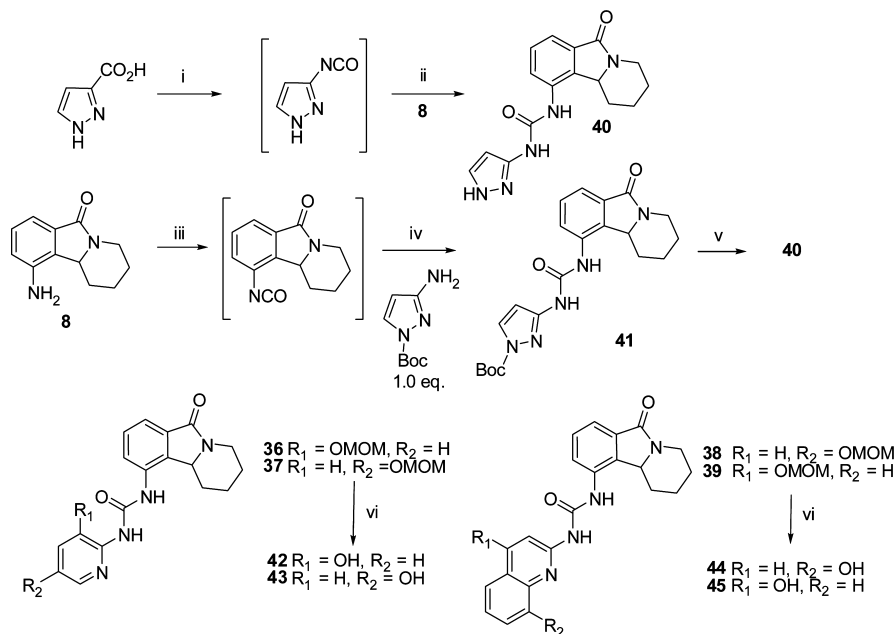
[a]Key: (i) and (ii) see also Scheme 3, **40** 4%; (iii) BTC (1.0 equiv), Et$_3$N (2.0 equiv), CH$_2$Cl$_2$, reflux, 5 h; (iv) N-1-Boc-3-aminopyrazole (1.0 equiv), CH$_2$Cl$_2$/pyridine 9/1, rt, 16 h, 56%; (v) aq NaOH (1 M)/THF 1/2, rt, 24 h, 66%; (vi) aq HCl 10%, acetone, reflux, 2 h, **42** 90%, **43** 92%, **44** 92%, **45** 95%.

Table 2. Selection of R Residue on Valmerins[a]

Entry	Valmerins	R	CDK5 IC$_{50}$ (µM)	GSK3α/β IC$_{50}$ (µM)	DYRK1A IC$_{50}$ (µM)
1	13		>10	>10	>10
2	14		>10	>10	>10
3	15		0.08	0.17	>10
4	16		0.07	0.51	>10
5	34		>10	0.75	>10
6	35		1.5	0.38	>10
7	28		0.43	0.76	>10
8	33		0.53	0.12	>10
9	29		1.7	0.13	2.4
10	40		0.17	0.47	>10
11	30		0.51	0.31	>10
12	26		2.7	0.33	>10
13	27		1.5	0.27	>10
14	32		16	3.5	>10
15	31		0.068	0.17	>10
16	44		0.7	0.15	>10
17	45		10	1.2	5.6

[a]Compounds with an IC$_{50}$ CDK5 < 100 nM or GSK3 < 1 µM are selected. Assays were performed in triplicate.

values lower than 100 nM. A bromine atom or hydroxy group could be indiscriminately placed in positions 2–4, but disubstitution led to a partial inactivation. In position 2, bulky and lipophilic piperidine or phenyl rings were partially tolerated; compounds 24 and 25 inhibited GSK3 in the submicromolar range.

Table 3. Selection of Valmerin Pyridine Ring Substituents[a]
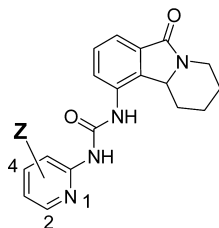
entry	valmerins	Z	CDK1 IC$_{50}$ (μM)	CDK5 IC$_{50}$ (μM)	GSK3α/β IC$_{50}$ (μM)	CK1 IC$_{50}$ (μM)	DYRK1A IC$_{50}$ (μM)
1	**15**	H	0.075	0.08	0.17	ND	>10
2	**18**	2-Br	ND	0.040	0.043	ND	3.4
3	**17**	3-Br	ND	0.13	0.076	ND	>10
4	**19**	4-Br	ND	0.025	0.022	1.3	7.6
5	**20**	2-F	ND	0.09	0.026	ND	3.5
6	**21**	3,5-diF	ND	0.26	0.2	>10	>10
7	**22**	2,3,4,5-tetrachloro	ND	10	4.3	ND	>10
8	**23**	5-OMe	ND	0.59	1.3	2.6	8.1
9	**24**	2-piperidinyl	ND	>10	0.36	>10	>10
10	**25**	3-phenyl	ND	4	0.14	>10	>10
13	**42**	3-OH	ND	0.037	0.051	1.5	1.8
14	**43**	5-OH	ND	1.3	4	≥10	>10

[a]Assays were performed in triplicate. ND: not determined. Compounds exhibiting an IC$_{50}$ CDK5 or GSK3 < 200 nM were selected.

Table 4. Protein Kinase Selectivity of Valmerin 15 in a Kinase Interaction Assay (KinomeScan)[a]

kinase	score	kinase	score	kinase	score	kinase	score
CDKL2	0	CSNK2A2	0.35	CDK2	0.9	KIT	2.8
DRAK1	0	L576P	0.35	V559D	1	KIT(D816V)	2.8
FLT3	0	RIOK1	0.35	PIP5K2B	1	TAK1	2.8
GSK3B	0	CDC2L5	0.4	CDK3	1.2	FLT3(K663Q)	2.9
JNK1	0	JNK2	0.4	CDK9	1.2	PKNB	3.1
MYLK4	0	PCTK2	0.4	PDGFRB	1.2	ABL1	3.2
PCTK1	0	TGFBR2	0.4	RSK2	1.2	TYK2	3.2
CDKL5	0.05	DRAK2	0.5	PFCDPK1	1.3	PRKD1	3.3
PFTK1	0.05	RIOK3	0.5	MEK5	1.4	PFTAIRE2	3.5
BIKE	0.1	CIT	0.6	CDKL1	1.6	TRKB	3.5
GSK3A	0.1	FLT3(	0.6	SRPK1	1.6	JAK1	3.8
JNK3	0.1	SNARK	0.6	MLCK	1.7	RSK1	4
CDK4-cyclinD3	0.15	MLK3	0.65	ICK	1.8	ARK5	4.3
CDKL3	0.15	PCTK3	0.7	EPHB6	2.2	FLT3	4.5
JAK3	0.15	YSK4	0.75	PRKD3	2.4	PKN2	4.5
ERK8	0.25	RSK4	0.85	STK36	2.5	FLT3(ITD)	4.6
CDK5	0.3	AURKC	0.9	ABL1	2.8	PRKD2	4.8

[a]Valmerin **15** was tested at a 10 μM concentration on a 442 kinase interaction panel. A semiquantitative scoring of this primary screen was obtained. This score relates to the probability of a hit rather than strict affinity. Scores >10, between 1−10 and <1, indicate that the probability of a hit being a false positive is <20%, <10%, and <5%, respectively. The best scores from 0 to 5 are presented. Full results are available in the Supporting Information (Table S1).

This pyridine variation completes our lead family. Searching for a compromise between CDK5 and GSK3 inhibition, it appeared that valmerins 18−20, 42 are the most interesting molecules of the substituted pyridinic series. However, the valmerin leading to the derivative 15 deserves considerable interest because of its ability to target with high efficacy the three main kinases involved in cell cycle and/or in growth control.

We also ran a semiquantitative kinase interaction assay (KinomeScan, Discoverx) of valmerin 15 at 10 μM on a 442 kinase panel. Results showed that CDKs (blue), CDK-like kinases (CDKLs) (orange), and GSK3 (green) are targeted in addition to quite a few other kinases (Table 4).

Molecular Modeling. The binding mode of our inhibitor 15 within GSK3 was elucidated using a docking model (Figure 3) and is characteristic of those found within the kinase family.[26] In this graphical representation, the valmerin 15 binds in the deep cleft between the two lobes of the catalytic core structure (the smaller N terminal domain at the top and the rich α helices C terminal domain below) and the extreme parts of the pyridine and piperidine rings are exposed to solvent.

Similarly to ATP, compound 15 binds the kinase active site forming two hydrogen bonds with the hinge region: the first one is present between the NH backbone of Val 135 and the urea's oxygen atom. The second one is realized between the oxygen of the Val 135 carbonyl group and the NH urea group
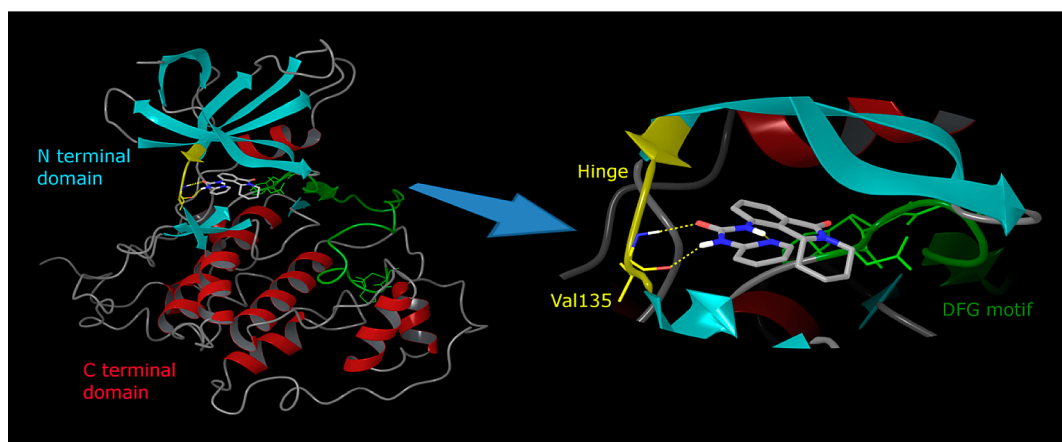
Figure 3. Binding mode of valmerin **15** within GSK3. Left: GSK3 protein from 2OW3 and **15** docked inside. Right: zoom on the active site. Hinge region was highlighted in yellow and the DFG motif of the activation loop is highlighted in green. Protein was represented as a ribbon diagram with the cartoon style and **15** exhibits tube representation (elements colored). Nonpolar hydrogens are not represented for clarity. H bonds are represented as dashed yellow lines.

Table 5. In Vitro Cell Effects of Selected Valmerins[a]
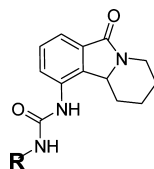
Entry	Valmerins	R	Human cell lines (IC$_{50}$ μM)						
			Huh7	Caco2	MDA-MB231	HCT 116	PC3	NCI-H727	Fibro.
1	**15**		0.24	0.42	0.32	0.15	0.22	0.29	0.89
2	**16**		0.83	1.84	1.50	0.69	0.65	1.00	2.38
3	**31**		2	1	3	1	2	3	4
4	**18**		>25	>25	>25	>25	>25	>25	>25
5	**19**		5	0.1	0.5	0.1	0.1	0.4	0.5
6	**20**		0.12	0.15	0.09	0.09	0.2	0.5	0.4
7	**42**		0.5	6	2	1	0.4	0.8	3

[a]Assays were performed in triplicate. Fibro represents skin fibroblast cell lines. Reference compounds used (not shown) were DMSO, Taxol, roscovitine, and doxorubicin.

again near the pyridine cycle of **15**. A supplementary hydrogen bond concerns **15** itself as it is an intra H bond connecting the second NH of urea with the nitrogen pyridine atom. This last hydrogen bond participates to the H bond pattern by orienting the urea group to the hinge residues.

In Vitro Cell Assays. To pursue our selection, all of the synthesized valmerins were evaluated against six representative human cancer cell lines (liver HuH7, colon Caco2 and HCT116, breast MDA-MB231, prostate PC3, and lung NCI-H727) as well as human normal diploid skin fibroblast cells. To
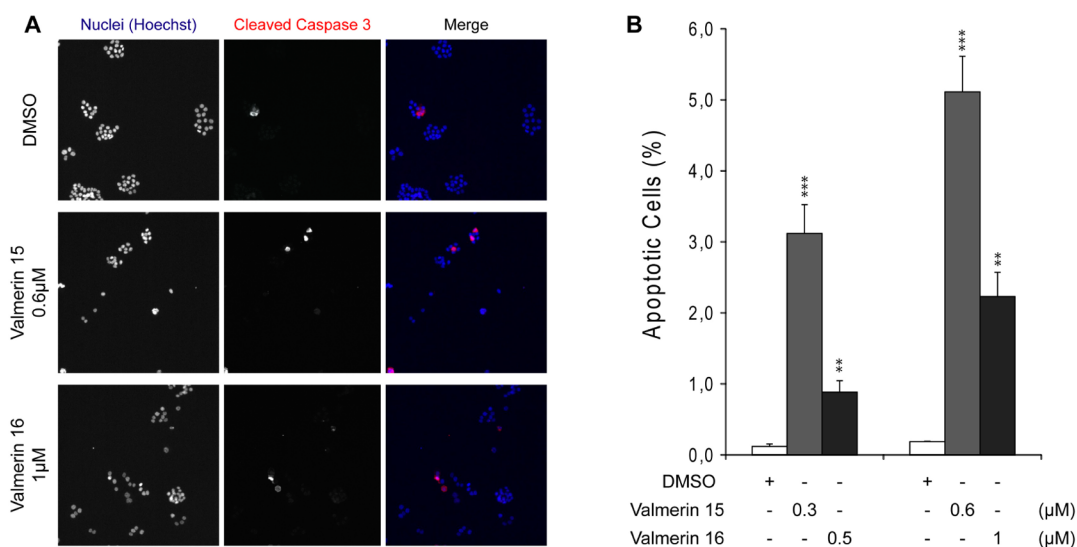
Figure 4. (A) Immunofluorescence labeling of cleaved (active) caspase 3 in HCT116 cells untreated (DMSO) or treated with valmerin **15** (0.6 μM) and valmerin **16** (1.0 μM) for 24 h. Nuclei were stained with Hoechst (blue), and apoptotic cells were immunostained with an antiactive caspase 3 antibody (red) (magnification, ×10). (B) Quantification of apoptotic cells. Apoptotic cells were calculated as the percent of active caspase 3-positive cells/total nuclei with the Cellomics High Content Imaging System. Data shown are the mean ± sem from a typical experiment performed in triplicate. **$P < 0.01$, ***$P < 0.001$, control cells vs treated cells.

simplify the presentation, we report in Table 5 the results for derivatives that showed submicromolar IC$_{50}$ values against CDKs and GSK3. All of the unselected molecules exhibited micromolar effects whatever the cell line (not shown); **18** precipitated during the cell effect measurements.

Effects on cells fully depended on the R substituent. Disappointingly, valmerin **31** only led to a micromolar effect on all the cancer cell lines tested. This compound was discarded because it appeared dramatically toxic on normal diploid fibroblast cells. Surprisingly, 4-bromopyridine derivative **19** affected all cell lines except the liver HuH7. This might be explained by the high expression of transporter proteins such as Pgp and MDRs, which may induce an early clearance of this target molecule in these cells.[27] The formation of an inactive metabolite through hepatic detoxification function cannot be ruled out.

The same variability in cell survival was amplified when considering compounds **42** and **16**. For compound **42**, submicromolar IC$_{50}$ values were obtained with HuH7, PC3, and NCI-H727 cells, while micromolar values were obtained with Caco2, MDA-MB231, HCT116 and with diploid fibroblasts; for compound **16**, no response was obtained with Caco2 and MDA-MB231 cell lines while all the others responded. Interestingly, these two cell lines carry mutations which alter growth controls, mainly those associated with Wnt-β catenin pathways which, therefore, drastically reduce the influence of GSK3 modulation, while the HCT 116 line, another colon cell line, has preserved part of these regulations.[28]

Nevertheless, three compounds **15**, **16**, and **20** emerged from this in vitro cell study. The best results were obtained with the HuH7, MDA-MB231, and HCT116 cell lines and IC$_{50}$ values were always lower than those observed with diploid fibroblasts. The best derivative is undoubtedly valmerin **15**. In this case, the three above-mentioned 3 cell lines were affected in the nanomolar range (240, 320, 150 nM, respectively) whereas normal fibroblasts were affected to a lower extent.

The strong cellular effect can be fully explained by multi kinase inhibition since the resulting effect on cells appeared as a pro-apoptotic effect. Indeed, additional studies performed on

valmerin **15** and **16** provide evidence supporting the idea that the decreased number of living cells induced by these compounds was mainly associated with strong induction of an apoptotic signal, principally induction of caspase 3 activity (Figure 4) as shown with the HCT116 cell line.

We therefore wondered whether this apoptotic effect could partly result from growth arrest induction and cell cycle inhibition. Progression into the cell cycle was estimated by using both S and M phase markers (Figure 5). Analyses led to detect a net decrease of cells engaged in the cell cycle, supporting the hypothesis of a blockage located at the entry or during the G1 phase. Further experiments on specific signaling pathways need to be performed to further confirm these conclusions. Again, valmerin **15** appeared more efficient than valmerin **16**.

In Vivo Assays. Valmerin **15** was selected for in vivo assays and was prepared in a gram scale. Tolerance was first evaluated in 6−8 week-old female NMRI mice (Janvier Laboratories). The up-and-down procedure was used with six animal per dose (0, 1, 5, and 10 mg/kg), the product was administered intraperitoneally and daily over 2 weeks, and the animals were monitored 2 weeks after the last administration. Daily observation over 14 consecutive days after product administration suggested good tolerance as shown by clinical signs, physical examination, body weight, and food consumption. Macroscopic examination of the organs at the end of the experiment showed no abnormalities and the blood formulation was normal.

Valmerin **15** partially slows down tumor growth in the HCT-116 mouse xenograft model. After 4 weeks of treatment, results showed a tumor reduction of 45.3% (Figure 6). At the end of the experiment, valmerin **15** had induced a 51% reduction in cecum BLI which correlates with the tumoral volume (Figure 6, right).

At necropsy, mesenteric nodes, liver and lung of each mouse were assessed on Φimageur to quantify the metastasis burden (Figure 7). There was no difference between control and Valmerin **15** treated mice in terms of mesenteric nodes or liver invasion, but only 1/9 treated mice had developed lung metastasis against 6/9 control mice. It seemed that Valmerin **15** had limited lung invasion.
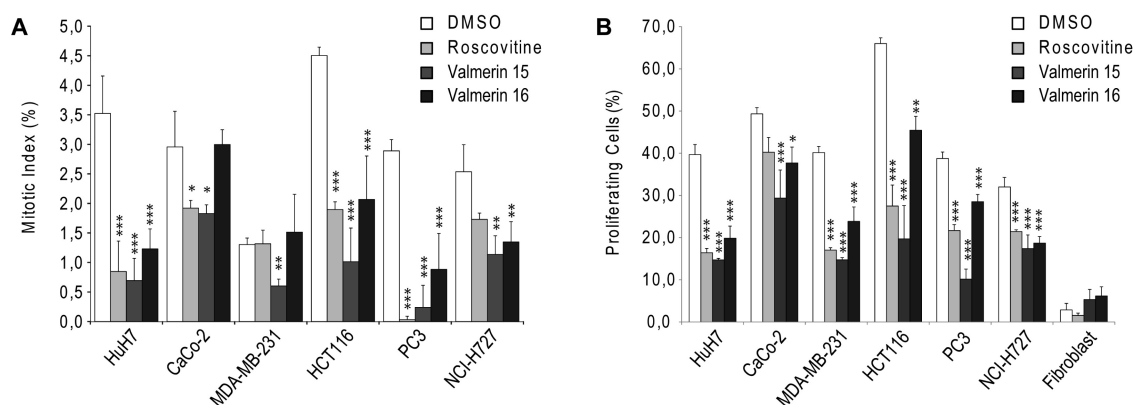
Figure 5. Effects of valmerins **15** and **16** on cell cycle progression. (A) Mitotic index. Different cell lines were treated with DMSO (0.4%) (control cells), roscovitine (20 μM), valmerin **15** (0.6 μM), and valmerin **16** (1 μM) for 24 h. Cells were fixed, and the mitotic index was determined using phospho-histone H3 detection. The number of dividing cells was calculated by using the Cellomics High Content Imaging System. Data shown are the mean $\pm$ SD from a typical experiment performed in triplicate. *$P < 0.05$, **$P < 0.01$, ***$P < 0.001$, control cells vs treated cells. (B) 5′-Bromo-2′-deoxyuridine (BrdU) incorporation. Different cell lines were treated with DMSO (0.4%) (control cells), roscovitine (20 μM), valmerin **15** (0.6 μM), and valmerin **16** (1 μM) for 48 h and pulsed with BrdU for 1 h 30. Cells were fixed and immunostained for BrdU incorporation. BrdU staining was measured by the Cellomics High Content Imaging System. Data shown are the mean $\pm$ SD from a typical experiment performed in triplicate. *$P < 0.05$, **$P < 0.01$, ***$P < 0.001$, control cells vs treated cells.
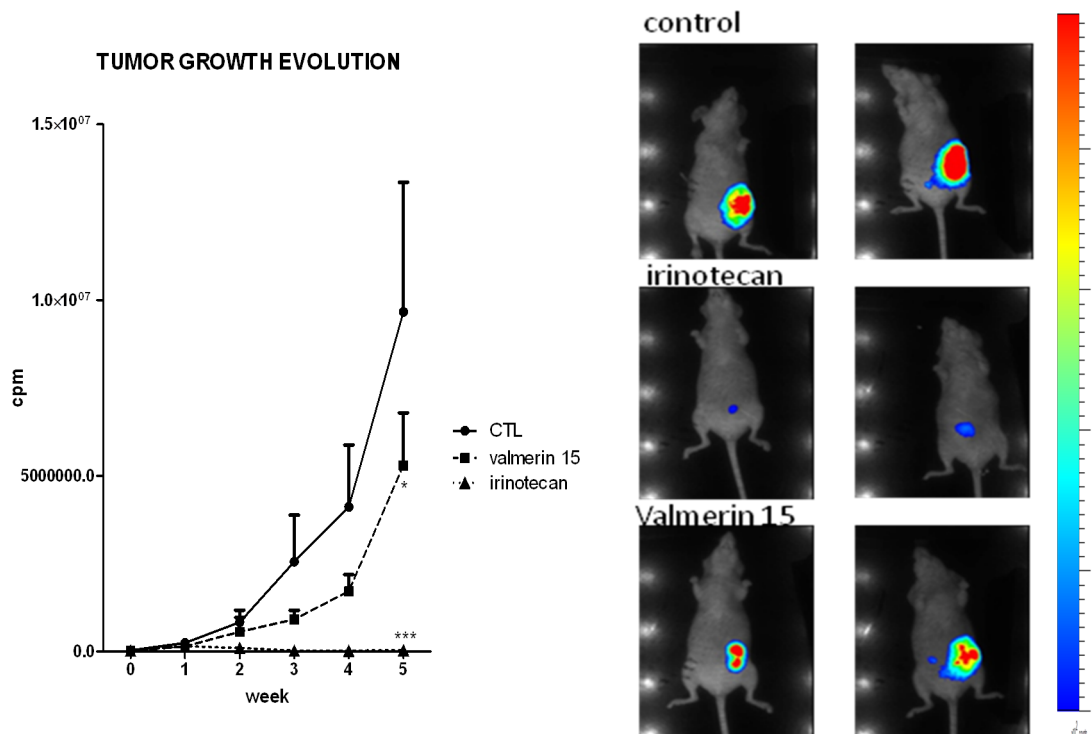
Figure 6. Left: in vivo valmerin **15** effects on tumor growth. Mice were assessed weekly using whole-body bioluminescent imaging to quantify relative amounts of tumor burden. Data are given as cpm mean +/− SD. $P < 0.05$: *, $p < 0.001$: ***. Right: 4 weeks after the beginning of treatment, BLI of two representative mice per group.

CONCLUSION

In this paper, we prepared valmerins, a new family containing the tetrahydropyrido[1,2-*a*]isoindone core. The fused heterocycle was prepared with a straightforward synthesis which was functionalized by a (het)aryl urea. Each final compound was evaluated against representative kinases and 12 valmerin inhibited CDK5 and GSK3 with IC$_{50}$ < 100 nM. A semi-quantitative kinase scoring confirmed that Valmerin **15** affected CDKs, CDK-like kinases (CDKLs), GSK3, and quite a few other kinases. Cellular screening on human cell lines (6 cancer cell lines and diploid fibroblasts) identified two stable lead compounds **15** and **16** with interesting submicromolar cellular effects. We have identified the cellular process which explains antiproliferative effects. Valmerins acted on proliferation and induced cell death by caspase 3 induction. At the end of our study, we investigated the in vivo potency of valmerin **15**. Mice exhibited good tolerance to our lead, which proved its efficacy and clearly blocked tumor growth. Valmerins appear as good candidates for further development as anticancer agents.
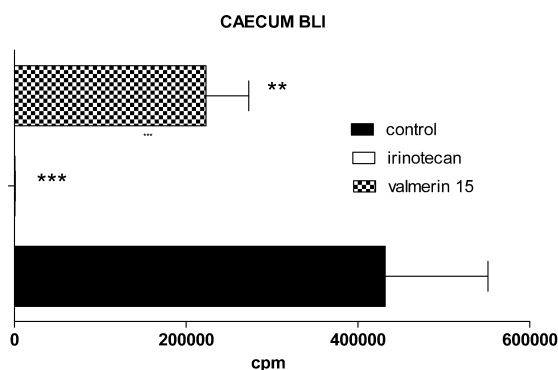
CAECUM BLI

	Control	Irinotecan	Valmerin 15
Mesenteric nodes	9 / 9	1 / 9	9 / 9
Liver metastasis	5 / 9	0 / 9	4 / 9
Lung metastasis	6 / 9	0 / 9	1 / 9

Figure 7. Left: Ex vivo cecum BLI at the end of the assay (left). The cecum BLI of all mice was quantified. Data are given as cpm mean +/− SD. $P < 0.01$: **, $p < 0.001$: ***. Right: At necropsy, the number of mice in each group with mesenteric nodes, liver and lung metastasis.

■ EXPERIMENTAL SECTION

Chemistry. ^{1}H NMR and ^{13}C NMR spectra were recorded on a Bruker DPX 250 or 400 MHz instrument using $CDCl_3$ or DMSO-d_6. The chemical shifts are reported in ppm (δ scale) and all coupling constants (J) values are in hertz (Hz). The splitting patterns are designated as follows: s (singlet), d (doublet), t (triplet), q (quartet), m (multiplet), and dd (doublet doublet). Melting points are uncorrected. IR absorption spectra were obtained on a Thermo-Nicolet equipped with an ATR Ge or Diamond equipment and values were reported in cm⁻¹. MS spectra (ion spray) were performed on a Perkin-Elmer Sciex PI 300. High-resolution mass spectra (HRMS) were performed on a Bruker maXis mass spectrometer by the "Fédération de Recherche" ICOA/CBM (FR2708) platform. Monitoring of the reactions was performed using silica gel TLC plates (silica Merck 60 F254). Spots were visualized by UV light at 254 and 356 nm. Chromatography columns were performed using silica gel 60 (0.063−0.200 mm, Merck). The purity was determined by using a VWR Hitachi HPLC equipped with a chiralpack IA column (250 × 4.6 mm). Mobile phase: A: 80% *n*-heptane. B: 20% ethanol. Flow 1 mL/min. Concentration 0.2 mg/mL in heptane/EtOH; inj 20 μL peaks were detected by UV absorption with a LaChrom Elite diode array detector L-2455 at 239, 249, and 254 nm. The HPLC profiles of all valmerins show purity up to ≥95%.

4-Nitro-2-(3-oxobutyl)isoindoline-1,3-dione (2). 3-Nitrophthalimide (5.0 g, 26.0 mmol), methyl vinyl ketone (2.8 mL, 3.3 mmol, 1.25 equiv), and Triton B (benzyltrimethylammonium hydroxide, 40% in methanol, 760 μL) in EtOAc (30 mL) were stirred at reflux overnight. Evaporation to dryness under reduced pressure and recrystallization from EtOH gives **2** as a yellow solid in 85% yield: mp 122−124 °C; ^{1}H NMR ($CDCl_3$, 250 MHz) δ 2.20 (s, 3H), 2.91 (t, J = 7.3 Hz, 2H), 3.98 (t, J = 7.3 Hz, 2H), 7.93 (dd, J = 7.1 Hz, J = 8.5 Hz, 1H), 8.07−8.19 (m, 2H); MS (IS) m/z 263.0 $[M + H]^+$; HRMS (ESI) calcd for $C_{12}H_{11}N_2O_5$ 263.06624, found 263.06631 $[M + 1]^+$.

2-(2-(2-Methyl-1,3-dioxolan-2-yl)ethyl)-4-nitroisoindoline-1,3-dione (3). A solution of the above ketone **2** (5.0 g, 19.0 mmol), ethylene glycol (2.0 mL, 38.0 mmol, 2.0 equiv), and PTSA·H₂O (21.0 mg, 0.1 mmol, cat.) in toluene (60 mL) was refluxed overnight with a Dean−Stark apparatus. The cooled solution was washed with aq satd NaHCO₃ (20 mL), and the organic layers were extracted with EtOAc, washed with brine (20 mL), dried over MgSO₄, filtered, and evaporated under reduced pressure. The crude material was recrystallized from ethanol to give **3** as a yellow crystal in 89% yield: mp 90−92 °C; ^{1}H NMR ($CDCl_3$, 250 MHz) δ 1.36 (s, 3H), 2.10 (t, J = 7.0 Hz, 2H), 3.86 (t, J = 7.0 Hz, 2H), 3.90−4.00 (m, 4H), 7.90 (dd, J = 7.4 Hz, J = 8.2 Hz, 1H), 8.05−8.17 (m, 2H); MS (IS) m/z 307 $[M + H]^+$, 324.0 $[M + NH_4]^+$; HRMS (ESI) calcd for $C_{14}H_{15}N_2O_6$ 307.09246, found 307.09244 $[M + H]^+$.

3-Hydroxy-2-(2-(2-methyl-1,3-dioxolan-2-yl)ethyl)-4-nitroisoindolin-1-one (4). To a solution of **3** (2.0 g, 6.5 mmol) in a mixture THF/MeOH (15/30 mL) at −30 °C was added NaBH₄ (700 mg, 19.5 mmol, 3.0 equiv) in portions. The mixture was stirred at this temperature for 15 min followed by TLC and then allowed to warm to

+10 °C. Aqueous satd NaHCO₃ (1 M, 40 mL) was added, and the organic layers were extracted successively with CH_2Cl_2 (10 mL) and EtOAc (10 mL). The combined organic layers were dried over MgSO₄, filtered, and concentrated in vacuum. Purification by column chromatography (CH_2Cl_2/MeOH 99/1) led to **4** as a white solid in 76% yield: mp 130−132 °C; ^{1}H NMR ($CDCl_3$, 250 MHz) δ 1.39 (s, 3H), 2.05−2.21 (m, 2H), 3.59−3.75 (m, 1H), 3.85−3.87 (m, 1H), 3.94−3.96 (m, 4H), 4.23 (d, J = 5.4 Hz, 1H), 6.46 (d, J = 5.4 Hz, 1H), 7.67−7.77 (m, 1H), 8.09 (dd, J = 0.7 Hz, J = 7.4 Hz, 1H), 8.32 (dd, J = 0.9 Hz, J = 8.2 Hz, 1H); MS (IS) m/z 309.0 $[M + H]^+$, 326.0 $[M + NH_4]^+$; HRMS (ESI) calcd for $C_{14}H_{17}N_2O_6$ 309.10811, found 309.10811 $[M + H]^+$.

10′-Nitro-3′,4′-dihydro-1′*H*-spiro[[1,3]dioxolane-2,2′-pyrido[2,1-*a*]isoindol]-6′(10b′*H*)-one (5). A solution of β-hydroxylactam **4** (500 mg, 1.62 mmol) and PTSA·H₂O (156 mg, 0.8 mmol, 0.5 equiv) in toluene (50 mL) was refluxed for 6 h with a Dean−Stark apparatus. After being cooled to room temperature, the mixture was washed three times with aq satd NaHCO₃ solution (45 mL), and the aqueous layers were extracted with EtOAc (3 × 20 mL). The combined organic layers were dried over MgSO₄, filtered, and evaporated under reduced pressure. Purification by column chromatography (CH_2Cl_2/MeOH 99.5/0.5) led to **5** as a yellow solid in 73% yield: mp 206−208 °C; ^{1}H NMR ($CDCl_3$, 250 MHz) δ 1.17 (t, J = 12.2 Hz, 1H), 1.65−1.95 (m, 2H), 2.61−2.78 (m, 1H), 3.33 (td, J = 4.2 Hz, J = 13.0 Hz, 1H), 3.96−4.31 (m, 4H), 4.55 (dd, J = 4.3 Hz, J = 13.4 Hz, 1H), 5.23 (dd, J = 3.3 Hz, J = 11.7 Hz, 1H), 7.70 (t, J = 7.8 Hz, 1H), 8.19 (d, J = 7.4 Hz, 1H), 8.37 (d, J = 8.1 Hz, 1H); MS (IS) m/z 291.0 $[M + H]^+$; HRMS (ESI) calcd for $C_{14}H_{15}N_2O_5$ 291.09754, found 291.09775 $[M + H]^+$.

10-Nitro-1,3,4,10b-tetrahydropyrido[2,1-*a*]isoindole-2,6-dione (6). A mixture of keto-protected compound **5** (2.0 g, 6.91 mmol) in an aq HCl solution (10%, 20 mL) and acetone (30 mL) was refluxed for 3 h. After cooling, acetone was removed under reduced pressure, and the resulting crude material was filtered, washed with water, and dried to give compound **6** as a yellow solid in 90% yield: mp 215−217 °C; ^{1}H NMR ($CDCl_3$, 400 MHz) δ 2.08 (dd, J = 11.7 Hz, J = 14.5 Hz, 1H), 2.52−2.72 (m, 2H), 3.38−3.55 (m, 2H), 4.76−4.82 (m, 1H), 5.39 (dd, J = 4.0 Hz, J = 11.6 Hz, 1H), 7.78 (t, J = 7.8 Hz, 1H), 8.25 (d, J = 7.4 Hz, 1H), 8.44 (d, J = 8.0 Hz, 1H); MS (IS) m/z 247.0 $[M + H]^+$; HRMS (ESI) calcd for $C_{12}H_{11}N_2O_4$ 247.07133, found 247.07150 $[M + H]^+$.

10-Amino-1,3,4,10b-tetrahydropyrido[2,1-*a*]isoindole-2,6-dione (7). To a solution of compound **6** (2.0 g, 8.0 mmol) in CH_2Cl_2 (100 mL) was added Pd (C) 10% (200 mg). After being stirred at room temperature under hydrogen atmospheric pressure for 16 h, the mixture was filtered through Celite. After being washed with MeOH (20 mL), the combined organic layers were evaporated under reduced pressure. Purification by column chromatography (CH_2Cl_2/MeOH 99/1) led to **7** as a yellow solid in 88% yield: mp 68−70 °C; ^{1}H NMR ($CDCl_3$, 400 MHz) δ 2.21 (dd, J = 12.2 Hz, J = 13.8 Hz, 1H), 2.47−2.65 (m, 2H), 3.16−3.21 (m, 1H), 3.32−3.40 (m, 1H), 3.90 (s, 2H), 4.66 (dd, J = 3.9 Hz, J = 11.9 Hz, 1H), 4.73−4.79 (m, 1H), 6.85 (dd,

J = 3.9 Hz, J = 4.9 Hz, 1H), 7.34−7.27 (m, 2H); MS (IS) m/z: 217.0 [M + H]⁺; HRMS (ESI) calcd for $C_{12}H_{13}N_2O_2$ 21709715, found 217.09739 [M + H]⁺.

10-Amino-1,2,3,4-tetrahydropyrido[2,1-*a*]isoindol-6(10b*H*)-one (8). Keto compound 7 (500 mg, 2.31 mmol) and hydrazine monohydrate (0.45 mL, 9.24 mmol, 4.0 equiv) were added to a solution containing sodium (160 mg, 6.93 mmol, 3.0 equiv) in diethylene glycol (9 mL). After the mixture was reluxed for 4 h at 190 °C, the reaction was found to be complete (TLC) and the mixture was cooled. CH₂Cl₂ (50 mL) was added, and the organic layer was washed with NaOH (20 mL, 1 M in water), dried over MgSO₄, filtered, evaporated, and purified by silica gel chromatography column (CH₂Cl₂/MeOH 99.5/0.5) to give the compound 8 as a yellow solid in 86% yield: mp 50−52 °C; ¹H NMR (CDCl₃, 250 MHz) δ 1.10−1.12 (m, 1H), 1.29−1.52 (m, 1H), 1.52−1.74 (m, 1H), 1.75−1.88 (m, 1H), 1.98−2.02 (m, 1H), 2.50 (dd, J = 3.2 Hz, J = 13.4 Hz, 1H), 2.96 (td, J = 3.5 Hz, J = 12.9 Hz, 1H), 3.79 (s, 2H), 4.23 (dd, J = 3.6 Hz, J = 11.7 Hz, 1H), 4.49 (dd, J = 4.9 Hz, J = 13.3 Hz, 1H), 6.80 (dd, J = 1.4 Hz, J = 7.3 Hz, 1H), 7.17 −7.35 (m, 2H); MS (IS) m/z 203.0 [M + H]⁺; HRMS (ESI) calcd for $C_{12}H_{15}N_2O_2$ 203.11789, found 203.11807 [M + H]⁺.

General Procedure a for Carboxylic Acids 9−12 Synthesis. The commercial hydroxycarboxylic acids (1.0 mmol) were dissolved in MeOH (50 mL), and thionyl chloride (2.0 mmol) was added dropwise at 0 °C. The reaction was warmed to room temperature and then refluxed overnight. After cooling, methanol was removed under reduced pressure and the residue was dissolved in a saturated aqueous NaHCO₃ (15 mL). The mixture was extracted with EtOAc (3 × 20 mL). After evaporation of the combined organic layer, the crude material was purified by flash chromatography on silica gel (CH₂Cl₂/MeOH 98/2) to give the desirable hydroxyesters. The previously obtained hydroxy esters (1.0 mmol) were added to a suspension of K₂CO₃ (2.0 mmol, 2.0 equiv) in dry acetone (20 mL). Chloromethyl methyl ether (1.5 mmol, 1.5 equiv) was dropwise added, and the mixture was stirred at 0 °C for 10 min and then heated at 70 °C for 12h. After the mixture was cooled to room temperature, water (15 mL) was added, and the organic material was extracted with EtOAc (3 × 25 mL). The combined organic layers were washed with H₂O (10 mL) and brine (10 mL) and dried (Na₂SO₄). After filtration and reduction of the volatiles under reduced pressure, the crude material was purified by flash chromatography on silica gel (CH₂Cl₂/MeOH 95/5) to give the desirable intermediates, which were next engaged in a last saponification step. The MOM protected esters (1.0 mmol) were dissolved in a THF/H₂O 1/1 (10 mL) mixture, and NaOH (1.2 mmol, 1.2 equiv) was added. The solution was stirred for 2 h at room temperature, and THF was removed under reduced pressure. The aqueous layer was acidified with acetic acid (50%) until pH 5−6 prior to extraction with EtOAc (3 × 10 mL). The combined organic layers were dried with anhydrous MgSO₄, filtered, and evaporated under reduced pressure to give the desired acids 9−12.

3-(Methoxymethoxy)picolinic Acid (9). The compound 9 was obtained following the general procedure *A* from the 3-hydroxypicolinic acid as a white solid in 75% yield: mp 208−210 °C; ¹H NMR (DMSO-d_6, 400 MHz) δ 3.36 (s, 3H), 5.17 (s, 2H), 7.15 (d, J = 4.4 Hz, J = 8.0 Hz, 1H), 7.40 (d, J = 8.0 Hz, 1H), 8.03 (d, J = 4.4 Hz, 1H); SM (IS) m/z 184.0 [M + H]⁺; HRMS (ESI) calcd for $C_8H_{10}NO_4$ 184.06043, found 184.06066 [M + H]⁺.

5-(Methoxymethoxy)picolinic Acid (10). The compound 10 was obtained following the general procedure A from the 5-hydroxypicolinic acid as a white solid in 77% yield: mp 212−214 °C; ¹H NMR (DMSO-d_6, 250 MHz) δ 3.42 (s, 3H), 5.36 (s, 2H), 7.58 (dd, J = 2.5 Hz, J = 8.7 Hz, 1H), 8.04 (d, J = 8.7 Hz, 1H), 8.42 (s, 1H), 12.88 (Sl, 1H); SM (IS) m/z 184.0 [M + H]⁺; HRMS (ESI) calcd for $C_8H_{10}NO_4$ 184.06043, found 184.06073 [M + H]⁺.

8-(Methoxymethoxy)quinoline-2-carboxylic Acid (11). The compound 11 was obtained following the general procedure *A* from the 8-hydroxyquinoline-2-carboxylic acid as a white solid in 70% yield: mp 148−150 °C; ¹H NMR (DMSO-d_6, D₂O, 400 MHz) δ 3.24 (s, 3H), 5.32 (s, 2H), 7.32 (d, J = 7.6 Hz, 1H), 7.48−7.61 (m, 2H), 8.18 (d, J = 8.5 Hz, 1H), 8.38 (d, J = 8.5 Hz, 1H); SM (IS) m/z 234.0 [M + H]⁺,

256.0 [M + Na]⁺; HRMS (ESI) calcd for $C_{12}H_{12}NO_4$ 234.07608, found 234.07615 [M + H]⁺.

4-(Methoxymethoxy)quinoline-2-carboxylic Acid (12). The compound 12 was obtained following the general procedure A from the 4-hydroxyquinoline-2-carboxylic acid as a white solid in 72% yield: mp > 260 °C; ¹H NMR (DMSO-d_6, D₂O, 250 MHz) δ 3.50 (s, 3H), 5.62 (s, 2H), 7.69−7.75 (m, 2H), 7.88 (t, J = 7.5 Hz, 1H), 8.13 (d, J = 7.5 Hz, 1H), 8.25 (d, J = 7.5 Hz, 1H); SM (IS) m/z 232.0 [M − H]⁻; HRMS (ESI) calcd for $C_{12}H_{11}NO_4Na$ 256.05803, found 256.05825 [M + H]⁺.

General Procedure B for Isocyanate Synthesis from Acids V. Under argon, a stirred solution of carboxylic acid **V** (0.37 mmol) and Et₃N (66 µL, 0.48 mmol, 1.3 equiv) in dry THF (7 mL) was cooled to −10 °C. Ethyl chloroformate (53 µL, 0.55 mmol, 1.5 equiv) was dropwise added, and the resultant mixture was stirred for 1 h. Afterward, a solution of sodium azide (40 mg, 0.63 mmol, 1.70 equiv) in water (2 mL) was slowly added and the reaction monitored by TLC. After completion (1 h), the reaction mixture was poured into ice−water (5 mL) and quickly extracted with EtOAc (3 × 10 mL). The combined organic layers were dried over MgSO₄, filtered, and carefully evaporated under reduced pressure. The crude acylazide was dissolved in dry toluene (20 mL) and refluxed for 1 h under argon to give the corresponding isocyanate which was used in the next step.

General Procedure C for Synthesis of Valmerins 13−40. Under argon, to the freshly prepared isocyanate was added the amine **8** (0.37 mmol, 1.0 equiv) in dry dioxane (7 mL). The reacting mixture was heated at 100 °C and next cooled at room temperature. After a careful evaporation of the volatiles (T < 40 °C), the dark residue was purified by silica gel chromatography column to afford the desired valmerins 13−40.

1-Cyclohexyl-3-(6-oxo-1,2,3,4,6,10b-hexahydropyrido[2,1-a]-isoindol-10-yl)urea (13). The compound 13 was obtained following the general procedures B and C from the cyclohexanecarboxylic acid and the amine 8 after purification by flash chromatography (CH₂Cl₂/MeOH 99/1) as a white solid in 86% yield: mp 240−242 °C; ¹H NMR (CDCl₃, 400 MHz,) δ 0.88−0.97 (m, 1H), 1.10−1.14 (m, 3H), 1.29−1.34 (m, 3H), 1.46−1.60 (m, 2H), 1.67 (d, J = 12.4 Hz, 2H), 1.75 (d, J = 10.4 Hz, 1H), 1.85−1.94 (m, 3H), 2.51 (d, J = 12.4 Hz, 1H), 2.90 (t, J = 12.4 Hz, 1H), 3.64 (d, J = 7.6 Hz, 1H), 4.40−4.49 (m, 2H), 5.55 (d, J = 7.6 Hz, 1H), 7.33 (d, J = 7.6 Hz, 1H), 7.46 (s, 1H), 7.51 (d, J = 7.6 Hz, 1H), 7.57 (d, J = 8.0 Hz, 1H); HRMS (ESI) calcd for $C_{19}H_{26}N_3O_2$ 328.20195, found 328.20249 [M + H]⁺; purity >99% by HPLC; tR =13.08 and 18.76 min; n-heptane/ethanol (8:2).

1-(6-Oxo-1,2,3,4,6,10b-hexahydropyrido[2,1-a]isoindol-10-yl)-3-phenylurea (14). The compound 14 was obtained following the general procedures B and C from the benzoic acid and the amine 8 after purification by flash chromatography (CH₂Cl₂/MeOH 98/2) as a white solid in 80% yield: mp 134−136 °C; ¹H NMR (CDCl₃, 400 MHz) δ 0.89−0.95 (m, 1H), 1.26−1.34 (m, 1H), 1.43−1.49 (m, 1H), 1.74 (d, J = 12.4 Hz, 1H), 1.84 (d, J = 10.4 Hz, 1H), 2.56 (d, J = 11.6 Hz, 1H), 2.90 (t, J = 11.6 Hz, 1H), 4.40−4.49 (m, 2H), 7.01 (t, J = 7.2 Hz, 1H), 7.22−7.26 (m, 2H), 7.30−7.36 (m, 3H), 7.52 (d, J = 7.2 Hz, 1H), 7.64 (d, J = 8.0 Hz, 1H), 8.15 (s, 1H), 8.31 (s, 1H); SM (IS) (m/z) 322.5 [M + H]⁺; HRMS (ESI) calcd for $C_{19}H_{20}N_3O_2$ 322.15500, found 322.15530 [M + H]⁺; purity >99% by HPLC; t_R =20.06 and 21.11 min; n-heptane/ethanol (8:2).

1-(6-Oxo-1,2,3,4,6,10b-hexahydropyrido[2,1-a]isoindol-10-yl)-3-(pyridin-2-yl)urea (15). The compound 15 was obtained following the general procedures B and C from the pyridine-2-carboxylic acid and the amine 8 after purification by flash chromatography (CH₂Cl₂/MeOH 97/3 + 1% Et₃N) as a white solid in 90% yield: mp 142−144 °C; ¹H NMR (DMSO-d_6, 400 MHz) δ 0.77−0.95 (m, 1H), 1.22−1.36 (m, 1H), 1.64−1.83 (m, 2H), 1.91 (d, J = 13.3 Hz, 1H), 2.72 (dd, J = 3.0 Hz, J = 12.6 Hz, 1H), 2.97−3.12 (m, 1H), 4.26 (dd, J = 4.4 Hz, J = 13.0 Hz, 1H), 4.59 (dd, J = 3.3 Hz, J = 11.5 Hz, 1H), 7.03−7.11 (m, 1H), 7.33 (d, J = 8.3 Hz, 1H), 7.38 (dd, J = 0.8 Hz, J = 7.4 Hz, 1H), 7.45 (t, J = 7.7 Hz, 1H), 7.74−7.85 (m, 1H), 8.23 (d, J = 8.0 Hz, 1H), 8.29 (d, J = 4.0 Hz, 1H), 10.00 (s, 1H), 11.16 (s, 1H); HRMS (ESI) calcd for $C_{18}H_{19}N_4O_2$ 323.1508, found 323.1495 [M + H]⁺; purity >99% by HPLC; t_R =14.40 and 17.74 min; n-heptane/ethanol (8:2).

1-(6-Oxo-1,2,3,4,6,10b-hexahydropyrido[2,1-a]isoindol-10-yl)-3-(pyrazin-2-yl)urea (16). The compound **16** was obtained following the general procedures B and C from the pyrazine-2-carboxylic acid and the amine **8** after purification by flash chromatography (CH₂Cl₂/MeOH 96/4) as a beige solid in 70% yield: mp 215−217 °C; ¹H NMR (DMSO-d_6, 400 MHz) δ 0.88 (qd, J = 3.0 Hz, J = 12.7 Hz, 1H), 1.16−1.33 (m, 1H), 1.64−1.72 (m, 1H), 1.76 (d, J = 15.0 Hz, 1H), 1.91 (d, J = 13.1 Hz, 1H), 2.63 (dd, J = 3.0 Hz, J = 12.6 Hz, 1H), 3.03 (td, J = 3.8 Hz, 12.8 Hz, 1H), 4.26 (dd, J = 3.8 Hz, J = 13.0 Hz, 1H), 4.56 (dd, J = 3.4 Hz, J = 11.5 Hz, 1H), 7.42 (dd, J = 1.0 Hz, J = 7.4 Hz, 1H), 7.47 (t, J = 7.7 Hz, 1H), 8.13 (dd, J = 1.0 Hz, J = 7.9 Hz, 1H), 8.29 (d, J = 2.7 Hz, 1H), 8.31−8.36 (m, 1H), 8.93 (d, J = 1.3 Hz, 1H), 9.81 (s, 1H), 10.05 (s, 1H); HRMS (ESI) calcd for C₁₇H₁₇N₅O₂Na 346.1280, found 346.1289 [M + Na]⁺; purity >99% by HPLC; t_R =14.27 and 17.99 min; n-heptane/ethanol (8:2).

1-(5-Bromopyridin-2-yl)-3-(6-oxo-1,2,3,4,6,10b-hexahydropyrido[2,1-a]isoindol-10-yl)urea (17). The compound **17** was obtained the general procedures B and C from the 5-bromopicolinic acid and the amine **8** after purification by flash chromatography (CH₂Cl₂/MeOH 99/1) as a beige solid in 66% yield: mp 225−227 °C; ¹H NMR (DMSO-d_6, 400 MHz) δ 0.77−0.93 (m, 1H), 1.20−1.33 (m, 1H), 162−1.82 (m, 2H), 1.90 (d, J = 12.6 Hz, 1H), 2.63 (dd, J = 2.7 Hz, J = 12.6 Hz, 1H), 3.00−3.11 (m, 1H), 4.25 (dd, J = 4.2 Hz, J = 13.0 Hz, 1H), 4.59 (dd, J = 3.2 Hz, J = 11.5 Hz, 1H), 7.39 (dd, J = 0.8 Hz, J = 7.4 Hz, 1H), 7.45 (t, J = 7.7 Hz, 1H), 7.50 (d, J = 8.9 Hz, 1H), 8.00 (dd, J = 2.5 Hz, J = 8.9 Hz, 1H), 8.14 (dd, J = 0.7 Hz, J = 7.9 Hz, 1H), 8.40 (d, J = 2.3 Hz, 1H), 10.00 (s, 1H), 10.25 (s, 1H); HRMS (ESI) calcd for C₁₈H₁₇N₄O₂NaBr 423.0433, found 423.0427 [M + Na]⁺; purity >98% by HPLC; t_R = 8.77 and 18.73 min; n-heptane/ethanol (8:2).

1-(6-Bromopyridin-2-yl)-3-(6-oxo-1,2,3,4,6,10b-hexahydropyrido[2,1-a]isoindol-10-yl)urea (18). The compound **18** was obtained the general procedures B and C from the 6-bromopicolinic acid and the amine **8** after purification by flash chromatography (CH₂Cl₂/MeOH 99/1) as a beige solid in 70% yield: mp 218−220 °C; ¹H NMR (DMSO-d_6, 400 MHz) δ 0.87 (qd, J = 3.1 Hz, J = 12.7 Hz, 1H), 1.20−1.34 (m, 1H), 1.61−1.81 (m, 2H), 1.89 (d, J = 13.0 Hz, 1H), 2.55−2.66 (m, 1H), 3.02 (td, J = 3.6 Hz, J = 12.9 Hz, 1H), 4.26 (dd, J = 3.6 Hz, J = 13.0 Hz, 1H), 4.56 (dd, J = 3.4 Hz, J = 11.5 Hz, 1H), 7.27 (dd, J = 1.4 Hz, J = 6.8 Hz, 1H), 7.38−7.43 (m, 1H), 7.46 (t, J = 7.7 Hz, 1H), 7.65−7.75 (m, 2H), 8.10 (dd, J = 0.7 Hz, J = 7.8 Hz, 1H), 9.28 (s, 1H), 10.04 (s, 1H); HRMS (ESI) calcd for C₁₈H₁₇N₄O₂NaBr 423.0433, found 423.0428 [M + Na]⁺; purity >99% by HPLC; t_R =10.31 and 13.46 min; n-heptane/ethanol (8:2).

1-(4-Bromopyridin-2-yl)-3-(6-oxo-1,2,3,4,6,10b-hexahydropyrido[2,1-a]isoindol-10-yl)urea (19). The compound **19** was obtained following the general procedures B and C from the 4-bromopicolinic acid and the amine **8** after purification by flash chromatography (CH₂Cl₂/MeOH 99/1) as a white solid in 80% yield: mp 244−246 °C; ¹H NMR (DMSO-d_6, 400 MHz) δ 0.82−0.93 (m, 1H), 1.19−1.30 (m, 1H), 1.64−1.77 (m, 2H), 1.90 (d, J = 12.0 Hz, 1H), 2.64 (dd, J = 4.0 Hz, J = 12.0 Hz, 1H), 2.99−3.06 (m, 1H), 4.25 (dd, J = 4.0 Hz, J = 12.0 Hz, 1H), 4.59 (dd, J = 4.0 Hz, J = 12.0 Hz, 1H), 7.30 (dd, J = 0.8 Hz, J = 8.0 Hz, 1H), 7.38−7.46 (m, 2H), 7.68 (s, 1H), 8.14−8.18 (m, 2H), 9.98 (s, 1H), 10.43 (s, 1H); HRMS (ESI) calcd for C₁₈H₁₈N₄O₂Br 401.06067, found 401.06076 [M + H]⁺; purity >99% by HPLC; t_R = 13.77 and 16.82 min; n-heptane/ethanol (8:2).

1-(6-Fluoropyridin-2-yl)-3-(6-oxo-1,2,3,4,6,10b-hexahydropyrido[2,1-a]isoindol-10-yl)urea (20). The compound **20** was obtained the general procedures B and C from the 6-fluoropicolinic acid and the amine **8** after purification by flash chromatography (CH₂Cl₂/MeOH 99/1) as a white solid in 70% yield: mp 244−246 °C; ¹H NMR (DMSO-d_6, 250 MHz) δ 0.70−1.03 (m, 1H), 1.12−1.40 (m, 1H), 1.52−1.72 (m, 1H), 1.76 (d, J = 14.1 Hz, 1H), 1.90 (d, J = 13.2 Hz, 1H), 2.57−2.75 (m, 1H), 3.02 (td, J = 3.5 Hz, J = 12.7 Hz, 1H), 4.26 (dd, J = 3.5 Hz, 13.0 Hz, 1H), 4.51 (dd, J = 3.3 Hz, J = 11.5 Hz, 1H), 6.77 (dd, J = 2.0 Hz, J = 7.9 Hz, 1H), 7.36−7.51 (m, 2H), 7.57 (dd, J = 2.1 Hz, J = 8.0 Hz, 1H), 7.94 (q, J = 8.2 Hz, 1H), 8.14 (dd, J = 1.2 Hz, J = 7.6 Hz, 1H), 9.33 (s, 1H), 9.92 (s, 1H); HRMS (ESI) calcd for

C₁₈H₁₇N₄O₂NaF 363.1233, found 363.1221 [M + Na]⁺; purity >99% by HPLC; t_R =11.39 and 13.45 min; n-heptane/ethanol (8:2).

1-(3,5-Difluoropyridin-2-yl)-3-(6-oxo-1,2,3,4,6,10b-hexahydropyrido[2,1-a]isoindol-10-yl)urea (21). The compound **21** was obtained following the general procedures B and C from the 3,5-difluoropicolinic acid and the amine **8** after purification by flash chromatography (CH₂Cl₂/MeOH 99/1) as a white solid in 73% yield: mp 256−258 °C; ¹H NMR (CDCl₃, 400 MHz) δ 1.06−1.16 (m, 1H), 1.39−1.51 (m, 1H), 1.64−1.76 (m, 1H), 1.85 (d, J = 12.5 Hz, 1H), 2.03 (d, J = 12.5 Hz, 1H), 2.65 (dd, J = 2.8 Hz, J = 12.8 Hz, 1H), 3.01 (td, J = 3.6 Hz, J = 12.8 Hz, 1H), 4.47 (dd, J = 3.6 Hz, J = 11.6 Hz, 1H), 4.54 (dd, J = 4.8 Hz, J = 12.8 Hz, 1H), 7.37−7.39 (m, 2H), 7.48 (t, J = 8.0 Hz, 1H), 7.66 (d, J = 7.5 Hz, 1H), 7.98 (d, J = 2.4 Hz, 1H), 8.11 (d, J = 8.0 Hz, 1H), 11.09 (s, 1H); HRMS (ESI) calcd for C₁₈H₁₇F₂N₄O₂ 359.13164, found 359.13141 [M + H]⁺; purity >99% by HPLC; t_R = 9.70 and 14.19 min; n-heptane/ethanol (8:2).

1-(6-Oxo-1,2,3,4,6,10b-hexahydropyrido[2,1-a]isoindol-10-yl)-3-(perchloropyridin-2-yl)urea (22). The compound **22** was obtained following the general procedures B and C from the 3,4,5,6-tetrachloropicolinic acid and the amine **8** after purification by flash chromatography (CH₂Cl₂/MeOH 99/1) as a beige solid in 60% yield: mp 246−248 °C; ¹H NMR (DMSO-d_6, 400 MHz) δ 0.84−0.92 (m, 1H), 1.15−1.29 (m, 1H), 1.64 (q, J = 12.8 Hz, 1H), 1.75 (d, J = 12.3 Hz, 1H), 1.88 (d, J = 13.0 Hz, 1H), 2.61 (d, J = 10.2 Hz, 1H), 3.02 (td, J = 3.8 Hz, J = 12.0 Hz, 1H), 4.25 (dd, J = 3.8 Hz, J = 12.6 Hz, 1H), 4.58 (dd, J = 3.3 Hz, J = 11.5 Hz, 1H), 7.44−7.49 (m, 2H), 7.97 (dd, J = 7.3 Hz, J = 1.2 Hz, 1H), 9.60 (d, J = 2.6 Hz, 2H); HRMS (ESI) calcd for C₁₈H₁₄N₄O₂NaCl₄ 480.9769, found 480.9789 [M + Na]⁺. Purity >97% by HPLC ; t_R =16.02 and 18.93 min ; n-heptane/ethanol (8:2).

1-(3-Methoxypyridin-2-yl)-3-(6-oxo-1,2,3,4,6,10b-hexahydropyrido[2,1-a]isoindol-10-yl)urea (23). The compound **23** was obtained following the general procedures B and C from the 3-methoxypicolinic acid and the amine **8** after purification by flash chromatography (CH₂Cl₂/MeOH 99/1) as a white solid in 70% yield: mp 202−204 °C; ¹H NMR (CDCl₃, 400 MHz) δ 1.03−1.13 (m, 1H), 1.38−1.50 (m, 1H), 1.65−1.76 (m, 1H), 1.83 (d, J = 12.8 Hz, 1H), 2.02 (d, J = 13.2 Hz, 1H), 2.81 (dd, J = 2.8 Hz, J = 12.8 Hz, 1H), 3.01 (td, J = 3.6 Hz, J = 12.8 Hz, 1H), 3.93 (s, 3H), 4.48 (dd, J = 3.6 Hz, J = 12.0 Hz, 1H), 4.54 (dd, J = 5.2 Hz, J = 13.2 Hz, 1H), 6.97 (dd, J = 5.2 Hz, J = 8.0 Hz, 1H), 7.12 (d, J = 8.0 Hz, 1H), 7.46 (t, J = 8.0 Hz, 1H), 7.59−7.62 (m, 2H), 7.79 (dd, J = 0.8 Hz, J = 5.2 Hz, 1H), 8.24 (d, J = 8.0 Hz, 1H), 11.86 (s, 1H); HRMS (ESI) calcd for C₁₉H₂₁N₄O₃ 353.16100, found 353.16082 [M + H]⁺. Purity >99% by HPLC ; t_R =15.63 and 14 min ; n-heptane/ethanol (8:2).

1-(6-Oxo-1,2,3,4,6,10b-hexahydropyrido[2,1-a]isoindol-10-yl)-3-(6-(piperidin-1-yl)pyridin −2-yl)urea (24). The compound **24** was obtained following the general procedures B and C from the 6-(piperidin-1-yl)picolinic acid and the amine **8** after purification by flash chromatography (CH₂Cl₂/MeOH 99/1) as a yellow solid in 81% yield: mp 234−236 °C; ¹H NMR (CDCl₃, 400 MHz) δ 0.94−1.05 (m, 1H), 1.34−1.38 (m, 1H), 1.54−1.65 (m, 7H), 1.77 (d, J = 12.8 Hz, 1H), 1.88 (d, J = 13.2 Hz, 1H), 2.43 (dd, J = 2.8 Hz, J = 12.8 Hz, 1H), 2.95 (td, J = 3.6 Hz, J = 13.2 Hz, 1H), 3.46−3.47 (m, 4H), 4.49 (dd, J = 3.6 Hz, J = 13.2 Hz, 1H), 4.69 (dd, J = 2.8 Hz, J = 12.8 Hz, 1H), 6.14 (d, J = 8.0 Hz, 1H), 6.31 (d, J = 8.0 Hz, 1H), 7.40−7.47 (m, 3H), 7.72 (d, J = 8.0 Hz, 1H), 8.40 (s, 1H), 11.59 (s, 1H); HRMS (ESI) calcd for C₂₃H₂₈N₅O₂ 406.22394, found 406.22375 [M + H]⁺. Purity >99% by HPLC ; t_R =12.93 and 19.84 min ; n-heptane/ethanol (8:2).

1-(6-Oxo-1,2,3,4,6,10b-hexahydropyrido[2,1-a]isoindol-10-yl)-3-(5-phenylpyridin-2-yl)urea (25). The compound **25** was obtained following the general procedures B and C from the 5-phenylpicolinic acid and the amine **8** after purification by flash chromatography (CH₂Cl₂/MeOH 99/1) as a white solid in 79% yield: mp >260 °C; ¹H NMR (DMSO-d_6, 400 MHz) δ 0.84−0.93 (m, 1H), 1.20−1.30 (m, 1H), 1.76 (d, J = 12.8 Hz, 2H), 1.91 (d, J = 12.8 Hz, 1H), 2.72 (d, J = 12.8 Hz, 1H), 2.95 (t, J = 12.4 Hz, 1H), 4.26 (d, J = 13.2 Hz, 1H), 4.61 (d, J = 12.8 Hz, 1H), 7.38−7.50 (m, 6H), 7.68 (d, J = 8.0 Hz, 2H), 8.11 (d, J = 8.4 Hz, 1H), 8.23 (d, J = 8.0 Hz, 1H), 8.59 (s, 1H), 10.01 (s, 1H), 11.07 (s, 1H); HRMS (ESI) calcd for C₂₄H₂₃N₄O₂ 399.1821,

found 399.1811 [M + H]⁺. Purity >99% by HPLC ; t_R =12.66 and 29.72 min ; n-heptane/ethanol (8:2).

11-(5-Methylisoxazol-3-yl)-3-(6-oxo-1,2,3,4,6,10b-hexahydropyrido[2,1-a]isoindol-10-yl)urea (26). The compound **26** was obtained the general procedures B and C from the 5-methylisoxazole-3-carboxylic acid and the amine **8** after purification by flash chromatography (CH$_2$Cl$_2$/MeOH 99/1) as a yellow solid in 72% yield: mp 156−158 °C; ¹H NMR (CDCl$_3$, 400 MHz) δ 1.03 (qd, J = 3.1 Hz, J = 12.8 Hz, 1H), 1.29−1.46 (m, 1H), 1.53−1.70 (m, 1H), 1.80 (d, J = 13.1 Hz, 1H), 1.94 (d, J = 13.3 Hz, 1H), 2.41 (s, 3H), 2.70 (d, J = 11.1 Hz, 1H), 2.98 (td, J = 3.2 Hz, J = 13.0 Hz, 1H), 4.49 (td, J = 4.0 Hz, J = 11.8 Hz, 2H), 6.12 (s, 1H), 7.44 (t, J = 7.8 Hz, 1H), 7.64 (d, J = 7.3 Hz, 1H), 7.99 (d, J = 7.9 Hz, 1H), 9.33 (s, 1H), 9.53 (s, 1H); HRMS (ESI) calcd for C$_{17}$H$_{18}$N$_4$O$_3$Na: 349.1277, found 349.1267 [M + Na]⁺; purity >95% by HPLC; t_R =13.13 and 24.25 min; n-heptane/ethanol (8:2).

1-(6-Oxo-1,2,3,4,6,10b-hexahydropyrido[2,1-a]isoindol-10-yl)-3-(5-phenylisoxazol-3-yl)urea (27). The compound **27** was obtained following the general procedures B and C from the 5-phenylisoxazole-3-carboxylic acid and the amine **8** after purification by flash chromatography (CH$_2$Cl$_2$/MeOH 99/1) as a white solid in 87% yield: mp 248−250 °C; ¹H NMR (DMSO-d$_6$, 400 MHz) δ 0.86 (qd, J = 2.9 Hz, J = 12.7 Hz, 1H), 1.17−1.34 (m, 1H), 1.54−1.71 (m, 1H), 1.76 (d, J = 12.5 Hz, 1H), 1.91 (d, J = 13.1 Hz, 1H), 2.61 (dd, J = 2.9 Hz, J = 12.5 Hz, 1H), 3.02 (td, J = 3.6 Hz, J = 12.8 Hz, 1H), 4.26 (dd, J = 3.6 Hz, J = 13.0 Hz, 1H), 4.52 (dd, J = 3.3 Hz, J = 11.5 Hz, 1H), 7.27 (s, 1H), 7.39−7.59 (m, 5H), 7.88 (dd, J = 1.7 Hz, J = 7.6 Hz, 2H), 8.04 (d, J = 7.7 Hz, 1H), 8.58 (s, 1H), 10.04 (s, 1H); HRMS (ESI) calcd for C$_{22}$H$_{20}$N$_4$O$_3$Na 411.1433, found 411.1414 [M + Na]⁺; purity >97% by HPLC; t_R =13.16, n-heptane/ethanol (8:2), no separation.

11-(6-Oxo-1,2,3,4,6,10b-hexahydropyrido[2,1-a]isoindol-10-yl)-3-(thiazol-4-yl)urea (28). The compound **28** was obtained following the general procedures B and C from the thiazole-4-carboxylic acid and the amine **8** after purification by flash chromatography (CH$_2$Cl$_2$/MeOH 99/1) as a yellow solid in 62% yield: mp 178−180 °C; ¹H NMR (CDCl$_3$, 400 MHz) δ 0.92−1.10 (m, 1H), 1.28−1.43 (m, 1H), 1.43−1.60 (m, 1H), 1.76 (d, J = 12.3 Hz, 1H), 1.88 (d, J = 12.2 Hz, 1H), 2.65 (d, J = 10.9 Hz, 1H), 2.91−2.97 (m, 1H), 4.38−4.57 (m, 2H), 7.11 (s, 1H), 7.41 (t, J = 7.8 Hz, 1H), 7.61 (d, J = 7.4 Hz, 1H), 7.96 (d, J = 7.8 Hz, 1H), 8.64 (d, J = 1.5 Hz, 1H), 9.68 (s, 1H); HRMS (ESI) calcd for C$_{16}$H$_{16}$N$_4$O$_2$NaS: 351.0892, found 351.0885 [M + Na]⁺; purity >96% by HPLC; t_R =20.45 and 29.15 min; n-heptane/ethanol (8:2).

1-(6-Oxo-1,2,3,4,6,10b-hexahydropyrido[2,1-a]isoindol-10-yl)-3-(2-(pyridin-4-yl)thiazol-4-yl)urea (29). The compound **29** was obtained following the general procedures B and C from the 2-(pyridin-4-yl)thiazol-4-carboxylic acid and the amine **8** after purification by flash chromatography (CH$_2$Cl$_2$/MeOH 99/1) as a orange solid in 60% yield: mp 152−154 °C; ¹H NMR (DMSO-d$_6$, 400 MHz) δ 0.85 (qd, J = 2.9 Hz, J = 12.7 Hz, 1H), 1.15−1.34 (m, 1H), 1.62 (q, J = 13.0 Hz, 1H), 1.76 (d, J = 12.6 Hz, 1H), 1.90 (d, J = 13.1 Hz, 1H), 2.62 (dd, J = 2.9 Hz, J = 12.6 Hz, 1H), 3.03 (td, J = 3.7 Hz, J = 12.9 Hz, 1H), 4.26 (dd, J = 3.7 Hz, J = 13.0 Hz, 1H), 4.50 (dd, J = 3.3 Hz, J = 11.5 Hz, 1H), 7.38 (dd, J = 0.8 Hz, J = 7.4 Hz, 1H), 7.45 (t, J = 7.7 Hz, 1H), 7.55 (s, 1H), 7.84 (dd, J = 1.6 Hz, J = 4.5 Hz, 2H), 8.11 (d, J = 7.2 Hz, 1H), 8.48 (s, 1H), 8.72 (dd, J = 1.5 Hz, J = 4.6 Hz, 2H), 10.10 (s, 1H); HRMS (ESI) calcd for C$_{21}$H$_{20}$N$_5$O$_2$S 406.1338, found 406.1343 [M + H]⁺; purity >96% by HPLC; t_R =8.20 and 28.09 min; n-heptane/ethanol (8:2).

1-(1-Methyl-1H-pyrazol-3-yl)-3-(6-oxo-1,2,3,4,6,10b-hexahydropyrido[2,1-a]isoindol-10-yl)urea (30). The compound **30** was obtained following the general procedures B and C from the 1-methyl-1H-pyrazole-3-carboxylic acid and the amine **8** after purification by flash chromatography (CH$_2$Cl$_2$/MeOH 99/1) as a white solid in 62% yield: mp 233−235 °C; ¹H NMR (DMSO-d$_6$, 400 MHz) δ 0.87 (dd, J = 23.0 Hz, J = 11.8 Hz, 1H), 1.25 (d, J = 12.6 Hz, 1H), 1.55−1.74 (m, 1H), 1.76 (d, J = 12.5 Hz, 1H), 1.92 (d, J = 13.1 Hz, 1H), 2.71 (d, J = 11.1 Hz, 1H), 3.03 (t, J = 11.6 Hz, 1H), 3.78 (s, 3H), 4.26 (d, J = 9.5 Hz, 1H), 4.52 (d, J = 8.9 Hz, 1H), 6.07 (s, 1H), 7.35 (d, J = 7.2 Hz, 1H), 7.43 (t, J = 7.7 Hz, 1H), 7.59 (s, 1H), 8.18

(d, J = 7.3 Hz, 1H), 9.21 (s, 1H), 9.42 (s, 1H); HRMS (ESI) calcd for C$_{17}$H$_{19}$N$_5$O$_2$Na 348.1436, found 348.1431 [M + Na]⁺; purity >97% by HPLC; t_R =11.05 and 31.89 min; n-heptane/ethanol (8:2).

1-(Isoquinolin-3-yl)-3-(6-oxo-1,2,3,4,6,10b-hexahydropyrido[2,1-a]isoindol-10-yl)urea (31). The compound **31** was obtained following the general procedures B and C from the 3-isoquinolin-3-carboxylic acid and the amine **8** after purification by flash chromatography (CH$_2$Cl$_2$/MeOH 99/1) as a white solid in 71% yield: mp > 260 °C; ¹H NMR (CDCl$_3$, 400 MHz) δ 1.10−1.20 (m, 1H), 1.43−1.49 (m, 1H), 1.72−1.88 (m, 2H), 2.07 (d, J = 13.2 Hz, 1H), 2.90 (dd, J = 2.8 Hz, J = 12.8 Hz, 1H), 3.04 (td, J = 3.2 Hz, J = 13.2 Hz, 1H), 4.54−4.60 (m, 2H), 7.38 (d, J = 6.0 Hz, 1H), 7.52 (t, J = 7.6 Hz, 1H), 7.65−7.68 (m, 2H), 7.79 (t, J = 7.6 Hz, 1H), 7.86 (d, J = 8.5 Hz, 1H), 8.08 (d, J = 6.0 Hz, 1H), 8.20 (d, J = 8.5 Hz, 1H), 8.34 (d, J = 8.0 Hz, 1H), 8.47 (s, 1H), 12.69 (s, 1H); HRMS (ESI) calcd for C$_{22}$H$_{21}$N$_4$O$_2$ 373.1665, found 376.1660 [M + H]⁺; purity >98% by HPLC; t_R =10.84 min; n-heptane/ethanol (8:2), no separation.

1-(Benzo[d]thiazol-2-yl)-3-(6-oxo-1,2,3,4,6,10b-hexahydropyrido-[2,1-a]isoindol-10-yl)urea (32). The compound **32** was obtained following the general procedures B and C from the acid **9** and the amine **8** after purification by flash chromatography (CH$_2$Cl$_2$/MeOH 99/1) as a yellow solid in 50% yield: mp 258−260 °C; ¹H NMR (DMSO-d$_6$, 400 MHz) δ 0.88 (q, J = 12.0 Hz, 1H), 1.15−1.32 (m, 1H), 1.64 (q, J = 13.0 Hz, 1H), 1.76 (d, J = 12.4 Hz, 1H), 1.90 (d, J = 12.8 Hz, 1H), 2.61 (d, J = 11.5 Hz, 1H), 3.01−3.07 (m, 1H), 4.26 (d, J = 9.2 Hz, 1H), 4.57 (d, J = 9.4 Hz, 1H), 7.26 (t, J = 7.5 Hz, 1H), 7.39−7.51 (m, 3H), 7.69 (d, J = 6.6 Hz, 1H), 7.93 (d, J = 7.7 Hz, 1H), 8.05 (d, J = 7.0 Hz, 1H), 9.07 (s, 1H), 11.19 (s, 1H); HRMS (ESI) calcd for C$_{20}$H$_{18}$N$_4$O$_2$NaS 401.1048, found 401.1066 [M + Na]⁺; purity >97% by HPLC; t_R =17.41 and 22.78 min; n-heptane/ethanol (8:2).

1-(2-Methylthiazol-4-yl)-3-(6-oxo-1,2,3,4,6,10b-hexahydropyrido-[2,1-a]isoindol-10-yl)urea (33). The compound **33** was obtained following the general procedures B and C from the acid **10** and the amine **8** after purification by flash chromatography (CH$_2$Cl$_2$/MeOH 99/1) as a yellow solid in 42% yield: mp 146−148 °C; ¹H NMR (CDCl$_3$, 400 MHz) δ 1.04 (q, J = 12.0 Hz, 1H), 1.31−1.47 (m, 1H), 1.48−1.62 (m, 1H), 1.78 (d, J = 12.6 Hz, 1H), 1.92 (d, J = 12.6 Hz, 1H), 2.71 (m, 4H), 2.95 (t, J = 12.0 Hz, 1H), 4.45 (dd, J = 3.5 Hz, J = 11.6 Hz, 1H), 4.51 (dd, J = 4.0 Hz, J = 13.2 Hz, 1H), 6.70 (s, 1H), 7.41 (t, J = 7.8 Hz, 1H), 7.62 (d, J = 7.3 Hz, 1H), 8.03 (d, J = 6.5 Hz, 1H), 9.30 (s, 2H); HRMS (ESI) calcd for C$_{17}$H$_{18}$N$_4$O$_2$NaS 365.1048, found 365.1062 [M + Na]⁺; purity >99% by HPLC; t_R =14.26 and 29.06 min; n-heptane/ethanol (8:2).

1-(6-Oxo-1,2,3,4,6,10b-hexahydropyrido[2,1-a]isoindol-10-yl)-3-pyrimidin-2-ylurea (34). The compound **34** was obtained following the general procedures B and C from the acid **12** and the amine **8** after purification by flash chromatography (CH$_2$Cl$_2$/MeOH 99/1) as a beige solid in 87% yield: mp 232−234 °C; ¹H NMR (DMSO-d$_6$, 400 MHz) δ 0.90 (dt, J = 12.0 Hz, J = 14.5 Hz, 1H), 1.25 (dd, J = 9.3 Hz, J = 13.3 Hz, 1H), 1.75 (t, J = 13.2 Hz, 2H), 1.92 (d, J = 13.1 Hz, 1H), 2.68 (d, J = 10.2 Hz, 1H), 2.96−3.11 (m, 1H), 4.27 (dd, J = 4.5 Hz, J = 12.8 Hz, 1H), 4.64 (dd, J = 3.2 Hz, J = 11.5 Hz, 1H), 7.20 (t, J = 4.9 Hz, 1H), 7.42 (d, J = 7.2 Hz, 1H), 7.48 (t, J = 7.7 Hz, 1H), 8.24 (d, J = 7.8 Hz, 1H), 8.70 (d, J = 4.9 Hz, 2H), 10.42 (s, 1H), 11.60 (s, 1H); HRMS (ESI) calcd for C$_{17}$H$_{18}$N$_5$O$_2$ 324.1461, found 324.1449 [M + H]⁺; purity >97% by HPLC; t_R =30.41 and 49.77 min; n-heptane/ethanol (8:2).

1-(6-Oxo-1,2,3,4,6,10b-hexahydropyrido[2,1-a]isoindol-10-yl)-3-(pyrimidin-4-yl)urea (35). The compound **35** was obtained following the general procedures B and C from the acid **12** and the amine **8** after purification by flash chromatography (CH$_2$Cl$_2$/MeOH 99/1) as a beige solid in 76% yield: mp 218−220 °C; ¹H NMR (DMSO-d$_6$, 400 MHz) δ 0.82−0.91 (m, 1H), 1.12−1.38 (m, 1H), 1.61−1.80 (m, 2H), 1.91 (d, J = 11.9 Hz, 1H), 2.64 (d, J = 10.9 Hz, 1H), 3.03 (t, J = 11.8 Hz, 1H), 4.26 (d, J = 9.6 Hz, 1H), 4.57 (d, J = 8.8 Hz, 1H), 7.40−7.50 (m, 2H), 7.54 (d, J = 5.4 Hz, 1H), 8.12 (d, J = 7.6 Hz, 1H), 8.58 (d, J = 5.6 Hz, 1H), 8.84 (s, 1H), 10.14 (s, 1H), 10.21 (s, 1H); HRMS (ESI) calcd for C$_{17}$H$_{18}$N$_5$O$_2$ 324.1461, found 324.1465 [M + H]⁺;

purity >96% by HPLC; t_R = 13.07 and 21.15 min; n-heptane/ethanol (8:2).

1-(3-(Methoxymethoxy)pyridin-2-yl)-3-(6-oxo-1,2,3,4,6,10b-hexahydropyrido[2,1-a]isoindol-10-yl)urea (36). The compound **36** was obtained following the general procedures B and C from carboxylic acid **9** and the amine **8** after purification by flash chromatography (CH$_2$Cl$_2$/MeOH 99/1) as a white solid in 73% yield: mp 182–184 °C; ^{1}H NMR (CDCl$_3$, 400 MHz) δ 1.03–1.19 (m, 1H), 1.42–1.55 (m, 1H), 1.70–1.75 (m, 1H), 1.86 (d, J = 12.8 Hz, 1H), 2.05 (d, J = 13.2 Hz, 1H), 2.84 (dd, J = 2.8 Hz, J = 12.8 Hz, 1H), 3.04 (td, J = 2.8 Hz, J = 12.8 Hz, 1H), 3.54 (s, 3H), 4.48 (dd, J = 3.2 Hz, J = 12.8 Hz, 1H), 4.54 (dd, J = 4.8 Hz, J = 13.2 Hz, 1H), 5.28 (s, 2H), 6.94 (dd, J = 4.8 Hz, J = 8.0 Hz, 1H), 7.43–7.49 (m, 2H), 7.60–7.62 (m, 2H), 7.85 (dd, J = 1.2 Hz, J = 8.0 Hz, 1H), 8.23 (d, J = 8.0 Hz, 1H), 11.85 (s, 1H); HRMS (ESI) calcd for C$_{20}$H$_{23}$N$_4$O$_4$ 383.1719, found 383.1704 [M + H]$^+$; purity >99% by HPLC; t_R =17.70 and 19.00 min; n-heptane/ethanol (8:2).

1-(5-(Methoxymethoxy)pyridin-2-yl)-3-(6-oxo-1,2,3,4,6,10b-hexahydropyrido[2,1-a]isoindol-10-yl)urea (37). The compound **37** was obtained following the general procedures B and C from carboxylic acid **10** and the amine **8** after purification by flash chromatography(CH$_2$Cl$_2$/MeOH 99/1) as a white solid in 78% yield: mp 202–204 °C; ^{1}H NMR (CDCl$_3$, 400 MHz) δ 1.04–1.14 (m, 1H), 1.39–1.47 (m, 1H), 1.65–1.76 (m, 1H), 1.84 (d, J = 12.8 Hz, 1H), 2.03 (d, J = 13.2 Hz, 1H), 2.81 (dd, J = 3.2 Hz, J = 12.8 Hz, 1H), 3.02 (td, J = 3.2 Hz, J = 12.8 Hz, 1H), 3.52 (s, 3H), 4.48 (dd, J = 3.2 Hz, J = 12.0 Hz, 1H), 4.55 (dd, J = 4.8 Hz, J = 13.2 Hz, 1H), 5.17 (s, 2H), 6.96 (d, J = 8.8 Hz, 1H), 7.46–7.50 (m, 2H), 7.63 (d, J = 8.0 Hz, 1H), 8.02 (s, 1H), 8.26 (d, J = 8.0 Hz, 1H), 9.36 (s, 1H), 11.78 (s, 1H); HRMS (ESI) calcd for C$_{20}$H$_{22}$N$_4$O$_4$Na 405.1539, found 405.1547 [M + Na]$^+$; purity >97% by HPLC; t_R =17.48 and 30.68 min; n-heptane/ethanol (8:2).

1-(8-(Methoxymethoxy)quinolin-2-yl)-3-(6-oxo-1,2,3,4,6,10b-hexahydropyrido[2,1-a]isoindol-10-yl)urea (38). The compound **38** was obtained following the general procedures B and C from carboxylic acid **11** and the amine **8** after purification by flash chromatography (CH$_2$Cl$_2$/MeOH 99/1) as a white solid in 75% yield: mp 226–228 °C; ^{1}H NMR (CDCl$_3$, 400 MHz) δ 0.96–1.06 (m, 1H), 1.31–1.39 (m, 1H), 1.46–1.56 (m, 1H), 1.78 (t, J = 16.5 Hz, 2H), 2.53 (d, J = 10.8 Hz, 1H), 3.00 (td, J = 3.2 Hz, J = 13.2 Hz, 1H), 3.42 (s, 3H), 4.54 (dd, J = 3.2 Hz, J = 13.2 Hz, 1H), 5.00 (dd, J = 3.2 Hz, J = 10.8 Hz, 1H), 5.34 (s, 2H), 7.14 (d, J = 8.8 Hz, 1H), 7.33–7.44 (m, 3H), 7.85 (t, J = 7.6 Hz, 1H), 7.77 (d, J = 7.6 Hz, 1H), 7.85 (d, J = 7.6 Hz, 1H), 8.09 (d, J = 8.8 Hz, 1H), 10.01 (s, 1H), 13.00 (s, 1H); HRMS (ESI) calcd for C$_{24}$H$_{25}$N$_4$O$_4$ 433.1876, found 433.1884 [M + H]$^+$; purity >96% by HPLC; t_R =12.85 and 21.95 min; n-heptane/ethanol (8:2).

1-(4-(Methoxymethoxy)quinolin-2-yl)-3-(6-oxo-1,2,3,4,6,10b-hexahydropyrido[2,1-a]isoindol-10-yl)urea (39). The compound **39** was obtained following the general procedures B and C from carboxylic acid **17** and the amine **8** after purification by flash chromatography (CH$_2$Cl$_2$/MeOH 99/1) as a white solid in 70% yield: mp > 260 °C; ^{1}H NMR (DMSO-d_6, 400 MHz) δ 0.85–1.01 (m, 1H), 1.16–1.32 (m, 1H), 1.53–1.79 (m, 3H), 2.52 (d, J = 10.4 Hz, 1H), 3.11 (td, J = 3.2 Hz, J = 13.2 Hz, 1H), 3.51 (s, 3H), 4.30 (dd, J = 3.2 Hz, J = 13.2 Hz, 1H), 4.82 (d, J = 10.4 Hz, 1H), 5.49 (s, 3H), 6.98 (s, 1H), 7.46–7.53 (m, 3H), 7.78 (t, J = 7.5 Hz, 1H), 7.90 (d, J = 7.5 Hz, 1H), 8.08 (d, J = 7.5 Hz, 1H), 8.28 (d, J = 7.5 Hz, 1H), 10.16 (s, 1H), 11.93 (s, 1H); HRMS (ESI) calcd for C$_{24}$H$_{25}$N$_4$O$_4$ 433.1876, found 433.1880 [M + H]$^+$; purity >98% by HPLC; t_R =8.31 and 9.91 min; n-heptane/ethanol (8:2).

1-(6-Oxo-1,2,3,4,6,10b-hexahydropyrido[2,1-a]isoindol-10-yl)-3-(1H-pyrazol-3-yl)urea (40). Compound **40** could be obtained as described in procedures B and C but in only a 4% yield. Alternatively, the following procedure led to **40** in a 66% yield. A mixture of **41** (60 mg, 0.146 mmol) and NaOH (1 M in water, 20 mL) in dry THF (10 mL) was stirred overnight at room temperature. The reaction mixture was extracted with hot EtOAc (3 × 20 mL). The combined organic layers were dried over MgSO$_4$ and reduced under reduced pressure to afford, after flash chromatography (CH$_2$Cl$_2$/MeOH 99/1),

the compound **40** as a white solid: mp 185–187 °C; ^{1}H NMR (DMSO-d_6, 400 MHz) δ 0.84 (qd, J = 12.8 Hz, J = 3.2 Hz, 1H), 1.16–1.34 (m, 1H), 1.56–1.83 (m, 2H), 1.90 (d, J = 13.2 Hz, 1H), 2.66 (d, J = 10.7 Hz, 1H), 3.01 (td, J = 3.0 Hz, J = 12.7 Hz, 1H), 4.26 (dd, J = 4.3 Hz, J = 13.1 Hz, 1H), 4.48 (dd, J = 3.2 Hz, J = 11.5 Hz, 1H), 6.20 (s, 1H), 7.35 (d, J = 7.2 Hz, 1H), 7.42 (t, J = 7.7 Hz, 1H), 7.63 (s, 1H), 8.12 (d, J = 7.9 Hz, 1H), 9.06 (s, 1H), 9.40 (s, 1H), 12.33 (s, 1H); HRMS (ESI) calcd for C$_{16}$H$_{18}$N$_5$O$_2$: 312.1461, found 312.1475 [M + H]$^+$; purity >97% by HPLC; t_R =12.56 and 15.98 min; n-heptane/ethanol (8:2).

3-[3-(6-Oxo-1,2,3,4,6,10b-Hexahydropyrido[2,1-a]isoindol-10-yl)-ureido]pyrazole-1-carboxylic Acid tert-Butyl Ester (41). To a stirred solution of **8** (140 mg ; 0.7 mmol) and Et$_3$N (0.2 mL, 2.0 equiv) in dry CH$_2$Cl$_2$ (10 mL) was added at 0 °C under Ar bis(trichloromethyl) carbonate (207 mg, 1.0 equiv). After 5 h at reflux, the reaction mixture was cooled to room temperature, and a solution of 3-aminopyrazole-1-carboxylic acid tert-butyl ester (128 mg, 1.0 equiv) in dry pyridine (1.2 mL) was added. The reaction mixture was stirred at room temperature for 18 h and then diluted with water (30 mL) and extracted with EtOAc (2 × 30 mL). The combined organic layers were successively washed with water (30 mL), dried over MgSO$_4$, and evaporated under reduced pressure to afford after silica gel column chromatography (CH$_2$Cl$_2$/MeOH 99/1) the compound **41** as a yellow solid in 56% yield: mp 136–138 °C; ^{1}H NMR (CDCl$_3$, 400 MHz) δ 0.98 (qd, J = 3.2 Hz, J = 12.7 Hz, 1H), 1.27–1.45 (m, 1H), 1.62 (s, 9H), 1.76 (d, J = 11.8 Hz, 1H), 1.85 (d, J = 13.0 Hz, 1H), 2.18 (s, 1H), 2.65 (s, 1H), 2.99 (t, J = 11.8 Hz, 1H), 4.49 (dd, J = 3.8 Hz, J = 13.0 Hz, 1H), 4.64 (d, J = 9.8 Hz, 1H), 6.38 (s, 1H), 7.42 (t, J = 7.8 Hz, 1H), 7.63 (d, J = 7.4 Hz, 1H), 7.91 (d, J = 2.9 Hz, 1H), 7.99 (s, 1H), 9.59 (s, 1H), 10.32 (s, 1H); HRMS (ESI) calcd for C$_{21}$H$_{25}$N$_5$O$_4$Na 434.1804, found 434.1791 [M + Na]$^+$.

General Procedure D. A mixture containing the protected urea (1 mmol), an aqueous solution of HCl (10%, 5 mL), and acetone (5 mL) was heated at reflux for 2 h. After cooling, acetone was removed under reduced pressure, and the resulting crude material was filtered, washed with water, and dried to give desired compound.

1-(3-Hydroxypyridin-2-yl)-3-(6-oxo-1,2,3,4,6,10b-hexahydropyrido[2,1-a]isoindol-10-yl)urea (42). The compound **42** was obtained following the general procedure D from compound **36** as a yellow solid in 90% yield: mp 190–192 °C; ^{1}H NMR (DMSO-d_6, 400 MHz) δ 0.76–0.84 (m, 1H), 1.18–1.27 (m, 1H), 1.58–1.68 (m, 1H), 1.74 (d, J = 12.8 Hz, 1H), 1.86 (d, J = 13.2 Hz, 1H), 2.69 (dd, J = 2.8 Hz, J = 12.8 Hz, 1H), 2.98 (td, J = 2.8 Hz, J = 12.8 Hz, 1H), 4.24 (dd, J = 4.0 Hz, J = 12.8 Hz, 1H), 4.66 (dd, J = 4.0 Hz, J = 12.8 Hz, 1H), 7.30 (dd, J = 6.4 Hz, J = 8.0 Hz, 1H), 7.45–7.52 (m, 2H), 7.84 (t, J = 9.6 Hz, 2H), 8.00 (dd, J = 1.2 Hz, J = 8.0 Hz, 1H), 10.57 (s, 1H), 10.86 (s, 1H), 12.73 (s, 1H); HRMS (ESI) calcd for C$_{18}$H$_{19}$N$_4$O$_3$ 339.1457, found 339.1441 [M + H]$^+$; purity >99% by HPLC; t_R =10.03 and 11.26 min; n-heptane/ethanol (8:2).

1-(5-Hydroxypyridin-2-yl)-3-(6-oxo-1,2,3,4,6,10b-hexahydropyrido[2,1-a]isoindol-10-yl)urea (43). The compound **43** was obtained following the general procedure D from compound **37** as a white solid in 92% yield: mp 206–208 °C; ^{1}H NMR (DMSO-d_6, 400 MHz) δ 0.79–0.89 (m, 1H), 1.20–1.27 (m, 1H), 1.63–1.75 (m, 2H), 1.88 (d, J = 13.2 Hz, 1H), 2.76 (dd, J = 2.8 Hz, J = 12.8 Hz, 1H), 3.01 (td, J = 3.2 Hz, J = 12.8 Hz, 1H), 4.25 (dd, J = 4.2 Hz, J = 13.2 Hz, 1H), 4.60 (dd, J = 3.2 Hz, J = 12.8 Hz, 1H), 7.33 (d, J = 8.8 Hz, 1H), 7.40–7.48 (m, 2H), 7.66 (d, J = 7.6 Hz, 1H), 7.89 (d, J = 2.8 Hz, 1H), 8.11 (d, J = 8.0 Hz, 1H), 10.34 (s, 2H), 11.01 (s, 1H); HRMS (ESI) calcd for C$_{18}$H$_{19}$N$_4$O$_3$ 339.1457, found 339.1451 [M + H]$^+$.

1-(8-Hydroxyquinolin-2-yl)-3-(6-oxo-1,2,3,4,6,10b-hexahydropyrido[2,1-a]isoindol-10-yl)urea (44). The compound **44** was obtained following the general procedure D from compound **38** as a white solid in 92% yield: mp 256–258 °C; ^{1}H NMR (DMSO-d_6, 400 MHz) δ 0.77–0.86 (m, 1H), 1.17–1.26 (m, 1H), 1.56–1.75 (m, 3H), 2.71 (d, J = 12.4 Hz, 1H), 3.04 (t, J = 12.4 Hz, 1H), 4.24 (dd, J = 2.8 Hz, J = 12.8 Hz, 1H), 4.79 (d, J = 12.8 Hz, 1H), 7.32–7.53 (m, 7H), 8.06 (d, J = 7.5 Hz, 1H), 8.57 (s, 1H), 11.27 (s, 2H); HRMS (ESI)

calcd for $C_{20}H_{21}N_4O_3$ 389.1614, found 389.1617 $[M + H]^+$; purity >96% by HPLC; t_R =18.34 min n-heptane/ethanol (8:2).

1-(4-Hydroxyquinolin-2-yl)-3-(6-oxo-1,2,3,4,6,10b-hexahydropyrido[2,1-a]isoindol-10-yl)urea (45). The compound **45** was obtained following the general procedure D from compound **39** as a white solid in 95% yield: mp > 260 °C; ^1H NMR (DMSO-d_6, 400 MHz) δ 0.77−0.86 (m, 1H), 1.21−1.27 (m, 1H), 1.58−1.85 (m, 3H), 2.78 (d, J = 10.5 Hz, 1H), 2.99 (td, J = 3.2 Hz, 13.2 Hz, 1H), 4.24 (dd, J = 3.2 Hz, J = 13.2 Hz, 1H), 4.63 (d, J = 10.8 Hz, 1H), 6.95 (s, 1H), 7.45−7.51 (m, 2H), 7.59 (t, J = 7.6 Hz, 1H), 7.88 (t, J = 7.6 Hz, 1H), 8.05 (d, J = 7.6 Hz, 1H), 8.13 (d, J = 8.4 Hz, 2H), 10.26 (s, 1H), 12.14 (s, 1H); HRMS (ESI) calcd for $C_{22}H_{21}N_4O_3$ 389.1614, found 389.1622 $[M + H]^+$; purity >99% by HPLC ; t_R =11.33 and 13.05 min; n-heptane/ethanol (8:2).

Biochemistry. *Buffers.* A: 10 mM $MgCl_2$, 1 mM EGTA, 1 mM DTT, 25 mM Tris-HCl pH 7.5, 50 μg heparin/mL. B: 60 mM ß-glycerophosphate, 30 mM p-nitrophenylphosphate, 25 mM Mops (pH 7.2), 5 mM EGTA, 15 mM $MgCl_2$, 1 mM DTT, 0.1 mM sodium vanadate, 1 mM phenylphosphate.

Kinase Preparations and Assays. Kinase activities were assayed in buffer A or C, at 30 °C, at a final ATP concentration of 15 μM. Blank values were subtracted and activities expressed in percent of the maximal activity, i.e., in the absence of inhibitors. Controls were performed with appropriate dilutions of DMSO. The kinase peptide substrates were obtained from Proteogenix (Oberhausbergen, France).

DYRK1A (human, recombinant, expressed in E. coli as a GST fusion protein) was purified by affinity chromatography on glutathione-agarose and assayed in buffer A (+ 0.5 mg BSA/mL) using Woodtide (KKISGRLSPIMTEQ) (1.5 μg/assay) as a substrate, in the presence of 15 μM $[\gamma^{-33}P]$ ATP (3,000 Ci/mmol; 10 mCi/mL) in a final volume of 30 μL.[30] After 30 min incubation at 30 °C, the reaction was stopped by harvesting onto P81 phosphocellulose papers (Whatman) using a FilterMate harvester (Packard) and were washed in 1% phosphoric acid. Scintillation fluid was added and the radioactivity measured in a Packard counter.

CDK5/p25 (human, recombinant) was prepared as previously described.[29] Its kinase activity was assayed in buffer B, with 1 mg of histone H1/mL.

GSK-3α/β[31] (porcine brain, native) was assayed in buffer A and using a GSK3 specific substrate (GS-1: YRRAAVPPSPSLSRHSSPHQ-pSEDEEE) (pS = phosphorylated serine).[32]

CK1δ/ε (porcine brain, native) was assayed in 3-fold diluted buffer B, using 25 μM CKS peptide (RRKHAAIGpSAYSITA), a CK1-specific substrate.[33]

Cell Biology Cell Culture and Survival Assay. Skin diploid fibroblastic cells were provided by BIOPREDIC International Co. (Rennes, France). HuH7, CaCo-2, MDA-MB-231, HCT116, PC3, and NCI-H727 cell lines were obtained from the ECACC collection. Cells were grown according to ECACC recommendations. The toxicity test of the compounds on these cells was as follows: 2×10^3 cells/well for HCT116 cell line, or 4×10^3 cells/well for the other cell lines, were seeded in 96 well plates. 24h after seeding, cells were exposed to increasing concentrations of the compounds (0.1−25 μM or 0.01−2.5 μM). After 48h of treatment, the cells were washed in PBS and fixed in cooled 90% ethanol/5% acetic acid for 20 min. Then, the nuclei were stained with Hoechst 3342 (Sigma). Image acquisition and analysis was performed using a Cellomics ArrayScan VTI/HCS Reader (Thermo Scientific).

Cell Proliferation. For BrdU incorporation, 2×10^3 cells/well for HCT116 cell line, or 4×10^3 cells/well for the other cell lines, were seeded in 96 well plates. Twenty-four hours after seeding, cells were exposed to the compounds. After 48 h of treatment, BrdU (Amersham) was added to the culture medium for 90 min. After fixation in 4% paraformaldehyde solution, cells were costained with Hoechst 3342 (Sigma) and anti-BrdU (Abcam). Image acquisition and analysis was performed using a Cellomics ArrayScan VTI/HCS Reader (Thermo Scientific). The percentage of proliferating cells was calculated by the amount of BrdU positive cells over the total Hoechst positive cells. For the mitotic index, 2×10^3 cells/well for HCT116 cell line, or 4×10^3 cells/well for the other cell lines, were seeded in 96 well plates.

Twenty-four hours after seeding, cells were exposed to the compounds. After 24 h of treatment, cells were fixed in 4% paraformaldehyde solution and then costained with Hoechst 3342 (Sigma) and antiphospho-Histone H3 (Ser10) (Millipore). Image acquisition and analysis was performed using a Cellomics ArrayScan VTI/HCS Reader (Thermo Scientific). The mitotic index was calculated as the percentage of mitotic cells identified by the phospho-histone H3-positive staining, vs the total Hoechst positive cells.

Apoptosis Analysis. A total of 2×10^3 HCT116 cells/well were seeded in 96 well plates. Twenty-four hours after cell seeding, cells were exposed to the compounds. After 24 h of treatment, cells were fixed in 4% paraformaldehyde solution and then stained for cleaved caspase 3 using the Cellomics Caspase 3 activation kit (Thermo-Scientific). Cells were stained according to the kit protocol. Image acquisition and analysis was performed using a Cellomics ArrayScan VTI/HCS Reader (Thermo Scientific).

Statistical Analysis. All data are expressed as mean ± SD, except if stated otherwise. We performed analysis of significance using a one-way ANOVA test followed by Bonferroni t test or using a Student's t test.

Orthotopic Colon Tumor Model. HCT-116-luc-cl5 is a luciferase expressing cell line that was derived from HCT-116 human adenocarcinoma cells by stable transfection of firefly luciferase gene. Cells were maintained in RPMI 1640 medium supplemented with 10% (v/v) fetal bovine serum, 2.0 mmol/L of glutamine and were grown in a humidified atmosphere at 37 °C with 5% CO_2. Female nude mice NMRI, 6−8 weeks old, were purchased from Janvier laboratories. Mice were bred and housed at INSERM, U892, University of Nantes, under the animal care license no. 44278. Mice were injected orthotopically with 2×10^6 HCT-116-luc cells in 30 μL of RPMI in the cecum wall. After 7 days, mice were randomized into three groups of nine mice. Valmerin group mice received intraperitoneally (i.p.) 10 mg/kg of valmerin **20** in 0.1 mL of vehicle (DMSO in 0.9% NaCl) three times a week for four weeks. The control group received 0.1 mL of vehicle with the same schedule. The third group was treated with reference drug irinotecan 15 mg/kg twice a week.

Bioluminescence Imaging (BLI). All mice were assessed weekly using whole-body bioluminescent imaging to quantify relative amounts of tumor burden (Φimageur ; BIOSPACE Lab, France). Each mouse was given potassium salt of D-luciferin (Interchim) at a dose of 150 mg/kg body weight by intraperitoneal injection. Bioluminescent images were collected in real time until a saturation plateau was reached. The amount of tumor burden was quantified as the relative amount of light produced from the luciferase activity in colon cancer cells and expressed in cpm using the Photovision+software (version 1.3 ; Biospace Lab). Mice were euthanized 5 weeks after inoculation of the tumor cells. At necropsy, ex vivo BLI measurement for each collected organ sample (including cecum, mesenteric nodes, liver, and lung) was performed. Drug efficacy was assessed as described below. Percent T/C in drug-treated versus control mice were expressed as follows: T/C (%) = 100 − (variation BLI treated mice/variation BLI control mice × 100). T/C (%) = 100 − (mean cecum BLI of treated mice/mean cecum BLI of control mice × 100).

Statistical analysis. Data were computed using Prism 5.0 software (Graphpad, La Jolla, CA). Groups were compared either by the 2 way ANOVA test or by the Kruskal−Wallis test, and $p < 0.05$ values were considered as indicative of significant differences between groups.

Molecular Modeling. *Docking Protocol.* All molecular modeling studies were performed with Schrodinger Molecular Modeling Suite 2012.[34] Maestro is the interface piloting the diverse modules. Glide was used to dock ligands.

Structure Preparation. The high-resolution crystal structure of GSK3 in complex with bis(indole)maleimide pyridinophane (BIM) was retrieved from the protein data bank,[35] under 2OW3 pdb code. The structure was prepared using the workflow Protein Preparation Wizard of the Schrodinger Molecular Modeling Suite 2012. A comparison of heavy atoms for the conformation of BIM cocrystallized and the conformation of BIM extracted and redocked within the receptor shows an rms derivation of 0.26 Å. Compound **15** was built within Marvin and was submitted to Corina,[36] a 3D structure

generator. The resulting structure became the starting point of our docking study.

■ ASSOCIATED CONTENT

Ⓢ Supporting Information

Additional characterization for compounds **2−45**, supplementary Table 1, Discoverx KinomeScan Selectivity Panel, and the ¹H and ¹³C NMR spectra for compounds **2−45**. This material is available free of charge via the Internet at http://pubs.acs.org.

■ AUTHOR INFORMATION

Corresponding Author

*Tel: 33 238 494 853. Fax: 33 238 417 281. E-mail: sylvain. routier@univ-orleans.fr.

Notes

The authors declare no competing financial interest.

■ ACKNOWLEDGMENTS

■ ABBREVIATIONS USED

GSK, glycogen synthase kinase; Triton B, benzyltrimethylammonium hydroxide; CSA, camphorsulfonic acid; PTSA, paratoluenesulfonic acid; BTC, bis(trichloromethyl) carbonate; DYRK, dual specificity tyrosine-phosphorylation-regulated kinase; CK, cyclin kinase; BrdU, 5′-bromo-2′-deoxyuridine; BLI, bioluminescence imaging; ATR: attenuated total reflection; IS, ion spray

■ REFERENCES

(1) Malumbres, M.; Carnero, A. Cell Cycle Deregulation: A Common Motif in Cancer. *Prog. Cell Cycle Res.* **2003**, *5*, 5−18.

(2) Malumbres, M.; Barbacid, M. Cell Cycle, CDKs and Cancer: A Changing Paradigm. *Nat. Rev. Cancer* **2009**, *9*, 153−166.

(3) Li, X.; Lu, F.; Tian, Q.; Yang, Y.; Wang, Q.; Wang, J. Z. Activation of Glycogen Synthase Kinase-3 Induces Alzheimer-like Tau Hyperphosphorylation in Rat Hippocampus Slices in Culture. *J. Neural Transm.* **2006**, *113*, 93−102.

(4) Ougolkov, A. V.; Billadeau, D. D. Targeting GSK-3: a Promising Approach for Cancer therapy. *Future Oncol.* **2006**, *2*, 91−100.

(5) (a) Wang, L. M.; Ren, D. M. Flavopiridol, the First Cyclin-Dependent Kinase Inhibitor: Recent Advances in Combination Chemotherapy. *Mini Rev. Med. Chem.* **2010**, *11*, 1058−1070. (b) Raje, N.; Hideshima, T.; Mukherjee, S.; Raab, M.; Vallet, S.; Chhetri, S.; Cirstea, D.; Pozzi, S.; Mitsiades, C.; Rooney, M.; Kiziltepe, T.; Podar, K.; Okawa, Y.; Ikeda, H.; Carrasco, R.; Richardson, P. G.; Chauhan, D.; Munshi, N. C.; Sharma, S.; Parikh, H.; Chabner, B.; Scadden, D.; Anderson, K. C. Preclinical Activity of P276−00, a Novel Small-Molecule Cyclin-Dependent Kinase Inhibitor in the Therapy of Multiple Myeloma. *Leukemia* **2009**, *5*, 961−970.

(6) Meijer, L., Bettayeb, K., Galons, H. Roscovitine (CYC202, Seliciclib). In Yue, E., Smith, P. J., Eds. *Monographs on Enzyme Inhibitors; Vol. 2. CDK Inhibitors and Their Potential as Anti-tumor Agents*; CRC Press: Boca Raton, 2006; Vol. 9, pp 187−226.

(7) Chu, X. J.; De Pinto, W.; Bartkovitz, D.; So, S. S.; Vu, B. T.; Packman, K.; Lukacs, C.; Ding, Q.; Jiang, N.; Wang, K.; Goelzer, P.; Yin, X.; Smith, M. A.; Higgins, B. X.; Chen, Y.; Xiang, Q.; Moliterni, J.; Kaplan, G.; Graves, B.; Lovey, A.; Fotouhi, N. Discovery of [4-Amino-2-(1-methanesulfonylpiperidin-4-ylamino)pyrimidin-5-yl](2,3-difluoro-6-methoxy phenyl)methanone (R547), a Potent and Selective Cyclin-Dependent Kinase Inhibitor with Significant *in Vivo* Antitumor Activity. *J. Med. Chem.* **2006**, *49*, 6549−6560.

(8) Tong, W. G.; Chen, R.; Plunkett, W.; Siegel, D.; Sinha, R.; Harvey, R. D.; Badros, A. Z.; Popplewell, L.; Coutre, S.; Fox, J. A.; Mahadocon, K.; Chen, T.; Kegley, P.; Hoch, U.; Wierda, W. G. Phase I and Pharmacologic Study of SNS-032, a Potent and Selective Cdk 2, 7, and 9 Inhibitor, in Patients with Advanced Chronic Lymphocytic Leukemia and Multiple Myeloma. *J. Clin. Oncol.* **2010**, *18*, 3015−3022.

(9) Baughn, L. B.; Di Liberto, M.; Wu, K.; Toogood, P. L.; Louie, T.; Gottschalk, R.; Niesvizky, R.; Cho, H.; Ely, S.; Moore, M. A.; Chen-Kiang, S. A Novel Orally Active Small Molecule Potently Induces G1 Arrest in Primary Myeloma Cells and Prevents Tumour Growth by Specific Inhibition of Cyclin-Dependent Kinase 4/6. *Cancer Res.* **2006**, *66*, 7661−7667.

(10) Byth, K. F.; Thomas, A.; Hughes, G.; Forder, C.; Mc Gregor, A.; Geh, C.; Oakes, S.; Green, C.; Walker, M.; Newcombe, N.; Green, S.; Growcott, J.; Barker, A.; Wilkinson, R. W. AZD5438, a Potent Oral Inhibitor of Cyclin-Dependent Kinases 1, 2, and 9, Leads to Pharmacodynamic Changes and Potent Antitumor Effects in Human Tumor Xenografts. *Mol. Cancer Ther.* **2009**, *7*, 1856−1866.

(11) Brown, A. P.; Courtney, C. L.; Criswell, K. A.; Holliman, C. L.; Evering, W.; Jessen, B. A. Toxicity and Toxicokinetics of the Cyclin-Dependent Kinase inhibitor AG-024322 in Cynomolgus Monkeys Following Intravenous infusion. *Cancer Chemother. Pharmacol.* **2008**, *62*, 1091−1101.

(12) Wyatt, P. G.; Woodhead, A. J.; Berdini, V.; Boulstridge, J. A.; Carr, M. G.; Cross, D. M.; Davis, D. J.; Devine, L. A.; Early, T. R.; Feltell, R. E.; Lewis, E. J.; McMenamin, R. L.; Navarro, E. F.; O'Brien, M. A.; O'Reilly, M.; Reule, M.; Saxty, G.; Seavers, L. C.; Smith, D. M.; Squires, M. S.; Trewartha, G.; Walker, M. T.; Woolford, A. J. Identification of *N*-(4-Piperidinyl)-4-(2,6-dichlorobenzoylamino)-1*H*-pyrazole-3-carboxamide (AT7519), a Novel Cyclin Dependent Kinase Inhibitor Using Fragment-Based X-Ray Crystallography and Structure Based Drug Design. *J. Med. Chem.* **2008**, *51*, 4986−4999.

(13) Jian, W.; Yamashita, H.; Levitt, J. M.; Lerner, S. P.; Sonpavde, G. Enzastaurin Shows Preclinical Antitumor Activity against Human Transitional Cell Carcinoma and Enhances the Activity of Gemcitabine. *Mol. Cancer Ther.* **2009**, *8*, 1772−1778.

(14) (a) Routier, S.; Ayerbe, N.; Mérour, J.-Y.; Coudert, G.; Bailly, C.; Pierré, A.; Pfeiffer, B.; Caignard, D.-H.; Renard, P. Synthesis and Biological Activity of 7-Azaindolocarbazoles. *Tetrahedron* **2002**, *58*, 6621−6630. (b) Routier, S.; Peixoto, P.; Mérour, J.-Y.; Coudert, G.; Bailly, C.; Pierré, A.; Léonce, S.; Caignard, D.-H. Synthesis and Biological Evaluation of New Naphthocarbazoles As Potential Anticancer Agents. *J. Med. Chem.* **2005**, *48*, 1401−1413. (c) Routier, S.; Mérour, J.-Y.; Dias, N.; Lansiaux, A.; Bailly, C.; Lozach, O.; Meijer, L. Synthesis and Biological Evaluation of Novel Phenylcarbazoles As Potential Anticancer Agents. *J. Med. Chem.* **2006**, *49*, 789−799. (d) Ayerbe, N.; Routier, S.; Gillaizeau, I.; Maiereanu, C.; Caignard, D. H.; Pierré, A.; Léonce, S.; Coudert, G. Synthesis and Biological Evaluation of Novel Benzodioxinocarbazoles (BDCZs) as Potential Anticancer Agents. *Bioorg. Med. Chem. Lett.* **2010**, *20*, 4670−4674.

(15) (a) Chiurato, M.; Routier, S.; Troin, Y.; Guillaumet, G. New Efficient Access to Fused Aryltetrahydroindolizinones via *N*-Acyliminium Intermediates. *Eur. J. Org. Chem.* **2009**, *18*, 3011−3021. (b) Chiurato, M.; Routier, S.; Troin, Y.; Guillaumet, G. New Efficient Access to Fused (Het)aryltetrahydroindolizinones via *N*-Acyl Iminium Intermediates. *Tetrahedron* **2010**, *66*, 4647−4653.

(16) (a) Honma, T.; Hayashi, Y.; Aoyama, T.; Hashimoto, N.; Machida, T.; Fukasawa, K.; Iwama, T.; Ikeura, C.; Ikuta, M.; Suzuki-Takahashi, I.; Iwasawa, Y.; Hayama, T.; Nishimura, S.; Morishima, H. Structure-Based Generation of a New Class of Potent Cdk4 Inhibitors: New de Novo Design Strategy and Library Design. *J. Med. Chem.*

2001, *44*, 4615−4627. (b) Honma, T.; Yoshizumi, T.; Hashimoto, N.; Hayashi, K.; Kawanishi, K.; Fukasawa, K.; Takaki, T.; Ikeura, C.; Ikuta, M.; Suzuki-Takahashi, I.; Hayama, T.; Nishimura, S.; Morishima, H. A Novel Approach for the Development of Selective Cdk4 Inhibitors: Library Design Based on Locations of Cdk4 Specific Amino Acid Residues. *J. Med. Chem.* **2001**, *44*, 4628−4640.

(17) Alsarabi, A.; Canet, J. L.; Troin, Y. Short Diastereoselective Synthesis of *cis*- and *trans*-Hexahydropyrido[2,1-*a*]isoindole Derivatives. *Tetrahedron Lett.* **2004**, *45*, 9003−9006.

(18) Valmerin is a nickmane which comes from the sentence "**Val**orisation des produits de la **Mer**" (see the Acknowledgments) and from the mane of some CDK inhibitors which use the suffix "In".

(19) Routier, S. ; Guillaumet, G., Meijer, L. ; Chiurato, M. ; Boulahjar, R. 10-Amino-1,2,3,4-tetrahydropyrido[2,1-*a*]isoindol-6-(10bH)-ones as CDK1, 5 and GSK-3 inhibitors. Patent WO 201050416; *Chem. Abstr.* **2009**, *153*, 431389.

(20) Gesson, J. P.; Jacquesy, J. C.; Rambaud, D. *α-N*-Acyliminium Ion - 2-Bromoalkene Cyclizations. *Tetrahedron* **1993**, *49*, 2239−2248.

(21) Lochead, A. W.; Proctor, G. R.; Caton, M. P. L. Use of Chloroalkenylamines for the Synthesis of 1-Azabicyclo[3.3.0]octane and 1-Azabicyclo[4.3.0]nonane Derivatives. *J. Chem. Soc., Perkin Trans. 1* **1984**, 2477−2489.

(22) Huang, M. *Contribution from the Chemical Laboratory of Harvard University* **1946**, *68*, 2487−2488.

(23) Löwik, D. W. P. M.; Tisi, L. C.; Murray, J. A. H.; Lowe, C. R. Synthesis of 6-Hydroxybenzothiazole-2-carboxylic Acid. *Synthesis* **2001**, 1780−1783.

(24) Brown, A. D. ; Ellis, D. ; Smith, C. R., Substituted Triazole Derivatives As Oxytocin Antagonists Their Preparation and Use against Sexual Dysfunction. Patent WO2005028452; *Chem. Abstr.* **2005**, *142*, 355271.

(25) Aakeröy, C. B.; Desper, J.; Levin, B.; Valdés-Martinez, J. Robust Building Blocks for Inorganic Crystal Engineering. *Inorg. Chim. Acta* **2006**, *359*, 1255−1262.

(26) (a) Zhang, H. C.; Boñaga, L. V. R.; Ye, H.; Derian, C. K.; Damiano, B. P.; Maryanoff, B. E. Novel Bis(indolyl)maleimide Pyridinophosphanes That Are Potent, Selective Inhibitors of Glycogen Synthase Kinase-3. *Bioorg. Med. Chem. Lett.* **2007**, *17*, 2863−2868. (b) Zhang, J.; Yang, P. L.; Gray, N. S. Targeting Cancer with Small Molecule Kinase Inhibitors. *Nature Rev. Cancer* **2009**, *9*, 28−39.

(27) Jacquemard, U.; Dias, N.; Lansiaux, A.; Bailly, C.; Logé, C.; Robert, J.-M.; Lozach, O.; Meijer, L.; Mérour, J. Y.; Routier, S. Synthesis of 3,5-Bis(2-indolyl)pyridine and 3-[(2-Indolyl)-5-phenyl]-pyridine Derivatives as CDK Inhibitors and Cytotoxic Agents. *Bioorg. Med. Chem.* **2008**, *16*, 4932−4953.

(28) Hoffman, K.; Franz, C.; Xiao, Z.; Mohr, E.; Serba, S.; Büchler, M. W..; Schemmer, P. Sorafenib Modulates the Gene Expression of Multi-drug Resistance Mediating ATP-Binding Cassette Proteins in Experimental Hepatocellular Carcinoma. *Anticancer Res.* **2010**, *30*, 4503−4508.

(29) Fukuyama, R.; Niculaita, R.; Ng, K. P.; Obusez, E.; Sanchez, J.; Kalady, M.; Aung, P. P.; Casey, G.; Sizemore, N.; Fukuyama, R. Mutated in colorectal Cancer, A Putative Tumor Suppressor for Serrated Colorectal Cancer, Selectively Represses Beta-Catenin-Dependent Transcription. *Oncogene* **2008**, *27*, 6044−6055.

(30) Debdab, M.; Carreaux, F.; Renault, S.; Soundararajan, M.; Fedorov, O.; Filippakopoulos, P.; Lozach, O.; Babault, L.; Tahtouh, T.; Baratte, B.; Ogawa, Y.; Hagiwara, M.; Eisenreich, A.; Rauch, U.; Knapp, S.; Meijer, L.; Bazureau, J.-P. Leucettines, a Class of Potent Inhibitors of cdc2-like Kinases and Dual Specificity, Tyrosine Phosphorylation Regulated Kinases Derived from the Marine Sponge Leucettamine B. Modulation of Alternative Pre-RNA Splicing. *J. Med. Chem.* **2011**, *54*, 4172−4186.

(31) Leclerc, S.; Garnier, M.; Hoessel, R.; Marko, D.; Bibb, J. A.; Snyder, G. L.; Greengard, P.; Biernat, J.; Mandelkow, E.-M.; Eisenbrand, G.; Meijer, L. Indirubins Inhibit Glycogen Synthase Kinase - 3β and CDK5/p25, Two Kinases Involved in Abnormal Tau Phosphorylation in Alzheimer's Disease - A Property Common to Most CDK Inhibitors? *J. Biol. Chem.* **2001**, *276*, 251−260.

(32) Primot, A.; Baratte, B.; Gompel, M.; Borgne, A.; Liabeuf, S.; Romette, J. L.; Costantini, F.; Meijer, L. Purification of GSK-3 by Affinity Chromatography on Immobilised Axin. *Protein Expr. Purif.* **2000**, *20*, 394−404.

(33) Reinhardt, J.; Ferandin, Y.; Meijer, L. Purification CK1 by Affinity Chromatography on Immobilised Axin. *Protein Expr. Puri.f* **2007**, *54*, 101−109.

(34) Maestro, version 9.3, Glide, version 5.8, Schrödinger, LLC, New York, 2012.

(35) http://www.rcsb.org/pdb/home/home.do.

(36) (a) Marvin 5.8.0, 2012, *ChemAxon* (http://www.chemaxon.com). (b) Sadowski, J.; Gasteiger, J. From Atoms and Bonds to Three-Dimensional Atomic Coordinates: Automatic Model Builders. *Chem. Reviews* **1993**, *93*, 2567−2581. (c) http://www.molecular-networks.com/products/corina.